Studies on the Initialization and Simulation of a Mature Hurricane Using A Variational Bogus Data Assimilation Scheme

Xiaolei Zou and Qingnong Xiao
Department of Meteorology
Florida State University
Tallahassee, FL 32306-4520

Submitted to JAS (17 August, 1998)
Revised (12 February, 1999)

ABSTRACT

A bogus data assimilation (BDA) scheme is presented and used to generate the initial structure of a tropical cyclone for hurricane prediction. It was tested on Hurricane Felix (1995) in the Atlantic ocean during its mature stage. The Penn State/NCAR nonhydrostatic mesoscale model version 5 (MM5) was used for both the data assimilation and prediction. It was found that a dynamically and physically consistent initial condition describing the dynamic and thermodynamic structure of a hurricane vortex can be generated by fitting the forecast model to a bogus surface low specified based on a few observed and estimated parameters. Through forecast model constraint, BDA is able to recover many of the structural features of a mature hurricane including a warm-core vortex with winds swirling in and out of the vortex center in the lower and upper troposphere respectively, the eyewall, the saturated ascent around the eye and descent or weak ascent in the eye, and the spiral cloud and rain bands. Satellite and radar data, if available, can be incorporated into the BDA procedure. We showed that satellite-derived water vapor winds have an added value for BDA to generate a more realistic initial vortex.

As a result of BDA, dramatic improvements occurred in the hurricane prediction of Felix. First of all, the initial adjustment and false spin-up of the model vortex were not observed because fields of model variables describing the BDA initial vortex are well-adapted to the forecast model. Secondly, the intensity forecast was greatly improved. The model correctly simulated the slight weakening of Hurricane Felix during the initial 12 h of model integration and then maintained a central pressure near 970 hPa thereafter, in good agreement with the observational estimates of the central pressure. Thirdly, the model captured the structures of the storm reasonably well. In particular, the model reproduced the ring of maximum winds, the eye, the eye-wall, and the spiral cloud-bands. Finally, improvement in the track prediction was also observed. The 24-h, 48-h, and 72-h forecast track errors with BDA were 76 km, 76 km and 84 km, respectively, comparing to the track errors of 93 km, 170 km and 193 km without BDA.

1 Introduction

Accurate prediction of hurricane track and intensity change is still a challenging task. The average position errors for NCEP (National Centers for Environmental Prediction) official hurricane track forecasts were about 160 km in 24-h and 250 km for 48-h forecast for seven Atlantic hurricanes (Kurihara et al., 1993). The skill of the hurricane intensity forecast varies from case to case and model to model and is probably more difficult than the track forecast. Many factors could be contributing to these difficulties in hurricane prediction. Lack of data over ocean, at both the tropical cyclone scale (providing an adequate description of the kinematic and thermodynamic structure of the storm) and the large-scale (describing large-scale circulation such as subtropical anticyclone accurately) in forming the model initial condition, deficiencies in the parameterization of physical processes (such as convection and air-sea interaction), as well as limited model resolution ($\geq$ 25 km) are some factors limiting the skill in the prediction of hurricanes. The first factor is the focus of this study.

Due to the lack of data, one of the major difficulties in numerical prediction of tropical cyclones is model initialization. Initial vortices provided by large-scale analysis from operational centers are often ill-defined, too weak, and sometimes misplaced. It was found necessary to introduce an initialization procedure to augment a more realistic initial vortex. This is usually carried out by implanting a synthetic vortex (the bogus vortex) into the large-scale analysis of the initial model state (Lord, 1991). The bogus vortex is specified based on the size of the cyclone (the radius of maximum winds), the position, and the intensity (the maximum vorticity). Many successful simulations, including prediction of hurricane movement and structure, were conducted using the bogus vortex for hurricane model initialization (Kurihara et al., 1990; Lord, 1991; Trinh and Krishnamurti, 1992). However, the detailed procedure of these bogus methods in constructing the model fields which are not directly related to the observed parameters, varies from one form to another. The nonlinear balance equation, gradient wind relation, geostrophic relation, hydrostatic relation, and other ad hoc assumptions are often used to derive one variable from another. How to generate all model fields of the initial vortex which are realistic, dynamically and physically consistent, and well-adapted to the prediction model have not been fully resolved

and is the focus of this study. an important and not fully resolved issue. The work by Kurihara et al. (1993) at the Geophysical Fluid Dynamics Laboratory (GFDL) represents a major step toward a better specification of an initial vortex for use in the hurricane prediction model. Model consistency and asymmetric structure of the initial vortex are emphasized in their initialization procedure and are obtained through a step-by-step procedure, which is briefly summarized as follows: (i) The vortex from the large-scale analysis is removed so that a smooth environmental field remains. (ii) An axisymmetric version of the hurricane prediction model is integrated while the model tangential wind component is forced to the target wind profile based on observational information to produce the symmetric part of the vortex. (iii) The symmetric flow produced in step (ii) is used to generate an asymmetric wind field by the time integration of a simplified barotropic vorticity equation. (iv) The mass field is then obtained based on the summation of symmetric and asymmetric flows and the divergence equation with an approximated time tendency through a diagnostic procedure. Numerical experiments conducted by Bender et al. (1993) confirmed that the modified scheme works successfully for the hurricane track and intensity prediction. The erratic movement and the less favorable structure in the early period of the model integration (the spin-up period of vortex adjustment), which often appear when NCEP global analysis is used, are alleviated.

These results indicate the importance of having a dynamically and thermodynamically consistent initial vortex that is compatible with the resolution and physics of the hurricane prediction model. A natural extension of GFDL's initialization ideas for the hurricane initialization is to use the full hurricane prediction model, instead of a series of simplified versions of the prediction model, as a strong dynamical constraint to generate all model fields in a 4-dimensional variational data assimilation (4D-Var) framework (Navon et al., 1992). The initial model fields generated by 4D-Var are dynamically and physically consistent and can be made close to a vortex field specified according to a few observed and estimated parameters. For example, a surface low can be formulated (using some empirical formula) from the known values of the central pressure (P_c), the maximum wind radius (R) and the location of the initial cyclone. The surface pressure data representing a spatial distribution

of the specified surface low can then be used as a set of "observations" for the forecast model to fit to. We call such a procedure "the bogus data assimilation" (BDA).

Of course, the BDA problem may be underdetermined with bogus data for only one variable to determine all the degree of model freedom. However, the underdetermined problem can be solved by introducing a background field (a short-term forecast), a penalty term and other available observational data. Recently, remote sensing instruments offered great promise for a much improved 3-dimensional description around and/or within a tropical cyclone. Examples of these observations are satellite-derived water vapor wind vectors (WVWVs), satellite-derived rain rates, satellite brightness temperatures, ozone data, and radar data. The benefit of using satellite observations for hurricane initialization and prediction was demonstrated by Krishnamurti et al. (1989, 1991, 1995). The fit of the model solution to the satellite observations was carried out through a physical initialization procedure after the bogus vortex was implanted into the initial condition. In BDA, the fit of the model solution to the bogus "observations" can be combined with a fit to other observations into a single procedure. The objective function that is minimized measures the distance (for example, a chosen inner product) between model solution and these bogused and actual observations. This flexibility of incorporating satellite and radar data in a hurricane initialization procedure is an additional advantage of the BDA scheme. In BDA, adjustments are made in all the model fields at the initial time when the model is forced to produce a solution close to the specified surface low and other available observations.

In this paper, we test the BDA scheme for a real-data hurricane prediction. The case chosen is Hurricane Felix, which occurred between 8-25 August 1995. For this case, both the satellite-derived WVWVs and the satellite GOES-8 and SSM/T-2 brightness temperature measurements are available around 15-16 August 1995 after Felix attained its maximum intensity. We will present results obtained by assimilating the bogus surface low only and both the bogus surface low and satellite WVWVs. Assimilation of satellite GOES-8 and SSM/T-2 brightness temperature observations for the same case will be presented in a future paper.

The Penn State/NCAR nonhydrostatic mesoscale model version 5 (MM5) is used for both the initialization and prediction. Success of MM5 in hurricane prediction has recently been

demonstrated by the work of Liu et al. (1997), in which a successful 72-h fine-scale simulation for Hurricane Andrew was made using MM5. The importance of having a proper initial vortex to start the MM5 model prediction was also indicated in their hurricane simulation. The initial vortex in their study was generated by making a 48-h model forecast starting from the initial vortex provided by the NCEP analysis at t_0, extracting the model-generated vortex at 48 h, and implanting it back to the NCEP analysis at t_0 according to the observed location. In addition, the initial relative humidity was increased by 85% everywhere over the ocean below 800 hPa outside the initial vortex and within the initial vortex from the surface to 300 hPa.

This study uses the same model for prediction but replaces the vortex implantation of Liu et al. (1997) with a new proposed BDA scheme. The MM5 forecast model is used in BDA as a strong model constraint to produce a dynamically and physically consistent initial vortex with the specified surface low in it. Once the initialization procedure is completed, a 72-h forecast is carried out to examine the impact of this initialization procedure on the hurricane prediction. The paper is organized as follows: A brief description of Hurricane Felix and its operational forecast results are summarized in section 2. The numerical model, initial conditions, vortex specification, and experiment design are described in section 3. In section 4, the dynamical and thermodynamical structure of the initial vortex generated by the BDA scheme is presented. Initial vortices, generated with only the specified surface low (with and without cloud water and rainwater) and with both the specified surface low and WVWVs are compared. The predicted storm tracks, intensity changes and storm structures with and without the BDA initialization will be shown in section 5. The paper concludes in section 6.

2 A brief description of Hurricane Felix

Hurricane Felix was initiated from a tropical wave that moved off the African coast on 6 August 1995. The post-analysis "best track" is shown in Fig. 1. Felix moved north and westward after it reached maximum intensity at 18 UTC 12 August. By 16 August, Felix assumed a general northwestward motion within 65 nm of Bermuda toward the North

Carolina coast. Felix turned northward on 17 August and then moved slowly northeastward on 18 August, instead of continuing the northwestward movement and making a landfall.

We choose a forecast period from 00 UTC 16 - 00 UTC 19 August 1995 to examine the model performance in predicting the north and northeastward turning of the hurricane track, the intensity change and the structures of Hurricane Felix. Although Felix never made landfall in the United States, some of the official forecasts and several of the track prediction models did indicate this possibility. If Felix had continued on the northwestward track onto the mid-Atlantic coast, considerable damage and loss of life would have been possible. An inaccurate hurricane landfall forecast will result in unnecessary threat and huge economic loss. We believe that avoiding a false prediction of hurricane landfall is as important as making a correct hurricane landfall forecast.

3 Experiment design

3.1 Model description

The Penn State/NCAR nonhydrostatic mesoscale model version 5 (MM5) is used for the numerical simulation of Hurricane Felix. It is run under two model configurations, one with a single domain at 30-km horizontal resolution (domain B) for the BDA procedure and the other with a movable, triply nested grid for the three-day forecasts. The grid system and physical options for the triply nested run are summarized in Table 1. There are 27 σ layers for all grid meshes with horizontal resolution of 90 km for the coarse mesh A, 30 km for the intermediate mesh B, and 10 km for the fine mesh C_i domain ($i = 1, 2, 3$ and 4, see Fig. 2). The domains A and B are fixed and the 10-km domain C_i moves along the hurricane track, with C_1, C_2, C_3, and C_4 for the forecast periods of 0-18 h, 18-42 h, 42-55 h and 55-72 h, respectively. The model physics include a cumulus parameterization scheme (Grell scheme or Kain-Fritsch scheme), the simple ice microphysics scheme (Dudhia scheme) or the mixed phase microphysics scheme (Reisner scheme), and the high-resolution planetary-boundary layer parameterization scheme (Blackadar scheme). The land surface temperature

is predicted using surface energy budget equations. A more detailed description of MM5 can be found in Dudhia (1993) and Grell et al. (1994).

Table 1: Grid system of the triply nested MM5

model domain	resolution (km)	dimension ($I \times J \times K$)	explicit moist scheme	cumulus parameterization
A	90	$45 \times 51 \times 27$	stable precipitation	Grell
B	30	$76 \times 85 \times 27$	Dudhia simple ice	Grell
C_1, C_2, C_3, C_4	10	$121 \times 121 \times 27$	Reisner mixed-phase	Kain-Fritsch

The BDA procedure carried out on domain B at 30 km resolution uses the physical processes included in the assimilation model. These processes are the same as those listed in Table 1 for domain B except that a bulk aerodynamic formulation of the planetary boundary layer is used. The MM5 adjoint modeling system (Zou et al., 1995; Zou et al., 1997) is employed in the BDA procedure.

3.2 Vortex specification

The bogused "observations" for the specified initial vortex consist of only the values of sea-level pressure (SLP) over a circular region of 300 km in radius. The surface low is specified based on the radius of maximum wind of the cyclone and its position and central pressure.

Fujita's formula (1952) is used as a basic reference for us to formulate axisymmetric SLP pattern of the bogused surface low. The formula is expressed as a function of r (radial distance from cyclone center) as follows:

$$P^{bogus}(r) = P_\infty - (P_\infty - P_c)/\{1 + (r/R_0)^2\}^{-1/2}, \tag{1}$$

where P_c and P_∞ are the value of the central pressure of the hurricane and an estimation of the SLP at an infinite distance, respectively. R_0 is a parameter with a dimension of length and is defined as the radius of maximum gradient of the SLP multiplied by $\sqrt{2}$.

At 00 UTC 16 August 1995, Hurricane Felix was located at 33.5°N, 70.1°W. The SLP at the hurricane center, P_c, was 963 hPa. The value of $R_0 = 150$ km is estimated based on the

NCEP large-scale analysis. The value of $P_\infty = 1035$ hPa is obtained by using an available ship report. A value of 1003.5 hPa surface pressure was observed at 35.1°N and 73.0°W by the ship LAVY4. By substituting this ship report of pressure as P^{bogus} in (??) we obtain $P_\infty = 1035$ hPa.

The values of bogus surface pressure P^{bogus} on all the model grid points within a circular region of 300 km radius (centered at the hurricane central position) are then calculated according to the equation (??). Figure 3 shows the distribution of these grids and the specified surface low. These bogus data are used as "observations" which will be assimilated into MM5 to generate a model initial state whose temperature, wind and moisture distributions within the initial vortex are dynamically and physically consistent with the bogus surface low.

3.3 Satellite WVWVs

With the deployment of a new generation of operational geostationary meteorological satellites, GOES-8/9, determination of wind fields over multiple tropospheric layers in cloud-free environments is possible through GOES-8/9 multispectral water vapor sensing capabilities (Velden et al., 1997). An example of such satellite-derived WVWV distribution during Felix is shown in Fig. 4. These are observations available at 00 UTC 16 August 1995. Also shown in Fig. 4 are the wind vectors based on the NCEP analysis, interpolated to the satellite observational locations. We found that the satellite-derived wind field (Fig. 4a) shows an upper-level cyclonic circulation near the center and an anticyclonic outflow away from the center. These features are not seen in the NCEP large-scale analysis (see Fig. 4c). In the low levels, however, satellite-derived wind does not seem to be as different from the NCEP analysis as in the upper layers. This and the WVWVS from only the cloud-free regions partially explain why assimilation of satellite WVWVs alone without a bogused surface low is not sufficient for a substantial improvement in the hurricane forecast.

3.4 The BDA procedure

Traditional tropical cyclone bogusing requires *a priori* specification of important structural aspects of the hurricane circulation (such as the tangential and radial wind components, the warm anomaly, and the moist core inside the hurricane). Although effort has been made to make such a specification more or less dynamically consistent by solving the balance equation, the vorticity advection equation, the hydrostatic equation and so on, complete coupling between various variables has not yet been achieved. The specified structure of one variable may not be used in a cause-effect way to explore the structure of another variable due to many of the *ad hoc* components existing in the bogusing procedure. In reality the dynamic and thermodynamic variables are completely interactive.

In the proposed BDA scheme, we choose to specify only one variable of the bogused vortex and let the complete forecast model spin up fields of other model variables. Since we have satellite WVWVs at the model initial time (i. e., 00 UTC 16 August 1995) which seem to contain useful information of wind vectors in the upper troposphere, the observed values of the central SLP of the hurricane are the most natural and simplest choice for bogus data. Values of central SLP of the hurricane can either be obtained by ship measurements or be estimated from satellite images (Dvorak, 1995). The central position of the hurricane can now be determined by airplane for operational use. Although such a choice of specifying a surface low is initially driven by these considerations related to the data availability and technical convenience, it is consistent with the statement of Willoughby (1995) that the atmosphere's adjustment of the balance wind and mass on a rotating Earth toward the low surface pressure attainable at equilibrium is the reason that tropical cyclones exist. Based on these considerations, we decided to test the model's ability to generate a 3-dimensional description of the structure of the initial vortex starting with a given surface low. The numerical model of a set of primitive equations with model dynamics and physics acts as a mechanism for all the model variables to response to the specified surface low.

More specifically, the hurricane initialization procedure is carried out by minimizing a cost function defined by either J_{BG} or J_{BGSAT}:

$$J_{BG}(\mathbf{x}_0) = \sum_{t_i} \sum_{i,j \in \mathcal{R}} (P - P^{bogus})^T W_P (P - P^{bogus}) + J_b, \qquad (2)$$

and

$$J_{BGSAT}(\mathbf{x}_0) = \sum_{t_i}\sum_{i,j\in\mathcal{R}}(P-P^{bogus})^T W_P (P-P^{bogus}) + \sum_{t_i}\sum_{\vec{r}_l}\Big(\left(H_l u - u^{SAT}(\vec{r}_l)\right)^T W_u \left(H_l u - u^{SAT}(\vec{r}_l)\right) + \left(H_l v - v^{SAT}(\vec{r}_l)\right)^T W_v \left(H_l v - v^{SAT}(\vec{r}_l)\right)\Big) + J_b \qquad (3)$$

where the summation over t_i is carried out at five minutes intervals over a half-hour window. $\mathcal{R}$ is a circular 2-dimensional domain of a 300 km (as a radius) circle centered at the hurricane center, (i,j) represents model horizontal grid points within $\mathcal{R}$ at the lowest σ level ($\sigma = 0.995$), $\vec{r}_l$ is the physical location in the 3D space representing satellite winds available at 00 UTC 16 August 1995 over the Atlantic ocean, and H_l is a linear interpolation scheme. W_P, W_u and W_v are diagonal weighting matrices and their values are determined empirically. Variables P, u and v represent SLP, zonal and meridional wind components, respectively. J_b represents a simple background term measuring the distance between the model state and the MM5 analysis based on the large-scale NCEP analysis. Only an approximated variances are included in the background weighting matrix.

One thing worth emphasizing is that the specified surface low data are assimilated every five minutes (i.e., at every time step) in a half-hour window. This is equivalent to assuming that the time tendency of the surface pressure is near zero. Such a constraint can also be incorporated by adding a penalty term to the cost function (see Zou et al., 1992; Zou et al., 1993).

The assimilation window used in the BDA scheme is very short (a few time steps). The computational cost is thus low comparing with a normal 4D-Var experiment (Courtier et al., 1994).

3.5 Initial conditions and experimental design

The model is initialized at 00 UTC 16 August 1995. The initial conditions for the control experiment (CTRL) are obtained from the NCEP 2.5° resolution global analysis, horizontally interpolated onto the regional domain for the mesh resolutions (see Table 1), and enhanced by rawinsondes and surface observations. An examination of the NCEP analysis reveals the

presence of a cyclonic circulation (Figs. 7a and c). However, the analysis fails to capture the right scale, correct location and sufficient intensity of the hurricane. Therefore, it is necessary to incorporate a vortex into the initial conditions with a realistic size, intensity, location and consistent dynamical and thermodynamical structure. This is carried out by a BDA procedure minimizing the objective functions defined either by (??) or by (??).

We present four 72-h simulations (listed in Table 2) which started from four initial conditions: (1) NCEP analysis; (2) the "optimal" initial condition obtained by the BDA scheme with P^{bogus} as the only "observations" using the MM5 assimilation model without including the moist variables q_c (cloudwater) and q_r (rainwater); (3) same as (2) except "observations" include both P^{bogus} and WVWVs; and (4) same as (2) except that q_c and q_r are included in MM5 assimilation model. As mentioned before, all the BDA experiments were carried out on domain B at 30-km resolution. Model simulations used a two-way interactive, movable, triply nested grid technique and were made starting with each of these four initial conditions. Coarser meshes provide the finer-meshes with time-dependent lateral boundary conditions while the finer-mesh solutions have feedback to coarser meshes every time step. The outermost lateral boundary conditions (for domain A) are specified by linearly interpolating the 12-h NCEP analyses. The initial condition on the domain C_1 (10-km resolution) are interpolated from the initial condition on domain B. These forecast experiments are designed to assess the potential values of the BDA procedure on hurricane prediction and the impact of satellite-derived WVWVs.

Table 2: Experimental name convention

experiment	"observations"	control variables for BDA	initial condition for 72-h forecast
CTRL			NCEP analysis
BG	P^{bogus}	u, v, w, T, q, p'	initial condition from BDA
BGSAT	P^{bogus} and WVWVs	u, v, w, T, q, p'	initial condition from BDA
BGM	P^{bogus}	u, v, w, T, q, p', q_c, q_r	initial condition from BDA

4 Initial structures within a mature hurricane generated by BDA

Minimization of J_{BG} converged in 30 iterations. During the minimization procedure, the model surface pressure was forced toward the bogused surface low, while the wind, temperature and moisture were free to develop an initial structure consistent with the surface pressure under the forecast model constraint. Figures 5-6 show the adjustments in the initial condition of the wind fields for the experiment BG, i.e., the differences between BG initial winds and the NCEP analyzed winds which were used as the guess field. We find that changes in the zonal wind (Du) above 200 hPa occur in the zonal direction, with a positive center located to the east and a negative center to the west of the vortex center (Fig. 5a). This positive/negative dipole rotates cyclonically with decreasing height. It rotated slightly less than 180° from top of the model to the bottom of the model. The positive/negative dipole in the low troposphere is not completely oriented in the west-east direction. The positive center is located to the southwest and the negative center to the northeast of the vortex center in the low levels (around and below 850 hPa, Fig. 5d). Minimum adjustments in the vertical are found around 500 hPa (Fig. 5c). Large changes in the meridional wind component are oriented in the north-south direction in the upper levels above 200 hPa, with a positive center to the north and a negative center to the south of the vortex center (Fig. 6a). A similar cyclonic rotation of slightly less than 180° from high levels to low levels is observed in the Dv distribution. Therefore, the Dv distribution in the low troposphere is not oriented in a complete north-south direction as in the upper levels. The maximum positive and negative adjustments are distributed in the direction from the southeast to the northwest (Fig. 6d).

These changes in both u- and v-components represent an outflow in the upper levels and a cyclonic inflow in the low level, which are induced by fitting the forecast model to the specified surface low (Fig. 7b and 7d). Compared with the NCEP large-scale analysis without BDA (Fig. 7a and 7c), the initial vortex in BG is much more compact and considerably more intense than the vortex in the global analysis. The asymmetric ring of maximum winds shows a more realistic distribution and is closer to the vortex center. The radius of maximum

winds decreases from 400 km in CTRL to about 110 km in BG. At 200 hPa, the difference between CTRL and BG are obvious. After BDA initialization, the divergence outflow rotates cyclonically from the eye and fans out anticyclonically around the two anticyclonic centers, one in the northwest of the vortex, and the other in the southeast of the vortex. Without the initialization, we observe a trough over the the vortex region at 200 hPa. Such a marked difference in the upper-layer flow near the vortex center may explain the long spin-up time (about 36 h) needed in CTRL for the model to generate a reasonable amount of rainfall and organized cloud patterns which are important for the storm intensification. In the low-level after BDA, we observe a cyclonic confluence of wind vectors into the central core, with a large cross-isobaric component (Fig. 7d). The NCEP analysis (Fig. 7c) has a low-level cyclonic flow but without a cross-isobaric component. The BG analysis reveals a strong 850 hPa wind of greater than 36.1 m s^{-1} to the northeast of the eye. The difference of the maximum wind speed between the BG and CTRL initial conditions is more than 10.9 m s^{-1}. We notice that, although a symmetric surface low is forced during the minimization procedure, the resulting wind speed distribution presents an asymmetric nature. This implies that the BDA scheme is able to generate the asymmetric structure of the initial vortex through the incorporation of observational information only sufficient for specifying a symmetric vortex structure. We believe that the vorticity advection by the background flow and the symmetric flow within the vortex, and influences of other non-symmetric components in the assimilation forecast model contributed to the generation of the asymmetric component in the initial vortex.

While the pressure gradient tends to draw air into the vortex center in the low troposphere, a systematic warming and moistening near the hurricane center results from such an air motion. Figure 8 shows the horizontal distribution of the adjustments in the initial condition of the temperature, the specific humidity and the vertical velocity at 850 hPa, as well as the surface pressure for the experiment BG. A nearly symmetric warming and deepening of the surface low are observed in the initial vortex region, with a maximum value of 10°C and -32 hPa, respectively (Fig. 8a and 8b). The moisture content is increased within the initial vortex and decreased in the southwest away from the center (Fig. 8c). Moisture excess in the vortex center exceeds 16 g kg^{-1}. The vertical velocity (Fig. 8d)

indicates a strong upward motion in the vortex region and a few banded regions of upward and downward motions around the periphery of the vortex.

In order to show the vertical distribution of the heating and moistening within the initial vortex generated by BDA, we plot in Fig. 9 a cross-section cutting through the center of the storm (see the line AB in Fig. 3) showing the vertical distribution of the temperature and specific humidity in the BG initial condition. We observe a consistent warming in all model levels. The maximum difference of about 13°C is located at 950 hPa. The increase of moisture content is also observed in all levels. The largest value of the specific humidity is 36 g kg^{-1}, located at 950 hPa. This appears to be too high a value and may not be supported by observations. As will be discussed later, a similar BDA procedure which includes cloudwater and rainwater as additional control variables (the experiment BGM) reduces the amount of increase in the specific humidity.

In summary, through forecast model constraint, variational assimilation of a bogused surface low alone is able to recover several structural features that a mature hurricane has (Figs. 5-9): a warm-core vortex with winds swirling in and out of the center in the low and upper troposphere respectively, and saturated ascent around the eye. We also notice that the horizontal distributions of the difference fields between BG and CTRL initial conditions for u, v and T resemble those that are produced by a single-observation experiment with the background error statistics specified in an operational 3D-Var data assimilation system (Parrish and Derber, 1992; Courtier et al., 1998). In addition, adjustments also occurred in the specific humidity field (Fig. 8c), which is usually not coupled with the wind and temperature in a 3D-Var system. This is one of the advantage of 4D-Var in which the specific humidity is coupled with wind, temperature and pressure fields through the advection and physical processes. The anticyclonic rotation with height of the bogus-surface-low induced positive and negative dipole structure of the u- and v adjustments with height (Figs. 6 and 7) reflects the nonlinear baroclinic and diabatic effects which may be difficult to be accounted for in a background error statistics.

We are aware that Felix was a mature hurricane at the initial time (00 UTC 16 August 1995) of our model simulations. Some of the structures characterizing a mature hurricane, such as the eye wall and the spiral cloud/rain bands, do not exist in the BG initial vortex.

These features, as we will see later, are defined more clearly (but not sufficiently with the BDA procedure being carried out at 30-km resolution in this study) when the satellite-derived WVWVs and the microphysical scheme are included into the BDA procedure.

In order to examine when and how the adjustment in the initial condition responded to the specified surface low during the BG minimization, we examine the root-mean-square (rms) differences of the following quantities:

$$Df^{(k)} = f^{(k)} - f^{(k-1)}$$

where f can be any of the model variables (u, v, T, q, p' and w) and k (=1, 2, ..., 10) is the number of iterations during the minimization procedure. Numerical results are shown in Fig. 10. We observe that the largest adjustment occurred in all the model fields at the 2nd iteration. The second largest adjustment occurred at the 5th iteration. Only small changes in the initial condition are noted after 7 iterations. For example, a total of 18.3 hPa deepening occurred in the first 4 iterations and an additional 13.1 hPa deepening occurred in the following 3 iterations (from the 5th to 7th iterations). In another word, 98% of the total deepening (32 hPa with 30 iterations) was completed in 7 iterations. Despite the large amount of computation of 4D-Var, the BDA runs quite effectively because of the use of a very short time window and the use of a bogus surface low being defined on all model grid points.

Examining the horizontal distribution of the sequential increments of wind, temperature and moisture at every iteration of the minimization procedure (figures omitted), we find that major adjustments occurred in two stages on two scales. Large-scale adjustments occurred before the 4th iteration (mainly at the 1st and 2nd iterations) and small-scale adjustments were obtained between 5th and 7th iteration (mainly at the 5th and 6th iterations). As an example, we show in Fig. 11 the distribution of $Du^{(2)}$, $Du^{(5)}$, $DT^{(2)}$ and $DT^{(5)}$ at 850 hPa. A zonal wind adjustment of about ± 6 m s^{-1} magnitude is obtained at both the 2nd and 5th iterations. The maximum value of $DT^{(2)}$ and $DT^{(5)}$ are 4°C and 2°C, respectively. We find that although the magnitude of the adjustments at the 5th iteration is similar to that at the 2nd iteration, the scale of the adjustment at the 5th iteration is smaller than that at the 2nd iteration.

We believe that the first major adjustment in the initial condition during the minimization of J_{BG} comes mainly from the dynamical constraint and the second major adjustment is associated with the latent heat release due to the heavy precipitation that occurred near the center of the initial vortex. To verify this, we examined the model predicted half-hour precipitation at each iteration and found that significant precipitation does not occur until the 5th iteration. Figure 12 plots the variation of the maximum values of the half-hour accumulated rainfall in the vortex region at each iteration. We observe that abrupt increase of the model precipitation, from less than 4 cm to more than 15 cm, occurred at both the 5th and 6th iterations.

Having examined the structures of the BG initial vortex, our next step is to see if the satellite-derived WVWVs have any added value and how they modify the initial vortex structure in BG. We find that the overall structures of the BGSAT vortex are similar to that of BG except that the BGSAT initial vortex has an eyewall more clearly defined than in BG. Figure 13 shows two cross-sections of the vertical velocity for both the BG and BGSAT vortices along the line CD shown in Fig. 3. A downward motion is observed in the center of the BGSAT vortex, in both the upper and low levels (Fig. 13b). In the BG vortex, the descent exists only in the upper levels near the top of the model. The upward motions on both sides of the vortex center are stronger in BGSAT than in BG. The differences in the vertical motion between BG and BGSAT are found to be related to the change of divergence field at 200 hPa in BGSAT (figure omitted), a direct result from the use of WVWVs.

In order to test the model's capability of generating spiral cloud/rain bands in the initial condition, we conducted an additional BDA experiment including a microphysics scheme in the assimilation model (the experiment BGM). The cloud (vertically integrated cloud water and rainwater) and the initial half-hour rainfall distributions for the BGM initial vortex are shown in Figure 14. It shows intense clouds in the center of the vortex, the cellular convection at the outer edge, and spiral cloud and rain bands around the central vortex. However, we notice that an echo-free eye is still missing in the central core. We attribute this to the use of a 30-km resolution which is still too coarse to resolve the hurricane eye adequately.

We notice that including the cloudwater and rainwater in the BDA procedure (BGM) reduces the amount of the increment in the specific humidity, which appears to be too high

in BG. Figure 15 presents a vertical cross-section (cutting through the center of the initial vortex from A to B in Fig. 3) of the specific humidity, cloudwater and rainwater in the BGM initial condition. Comparing Fig. 15a with Fig. 9b, we find that the maximum value of the specific humidity in the BG initial vortex is reduced from 36 g kg^{-1} in BG (Fig. 9b) to 32 g kg^{-1} in BGM (Fig. 15a). Another distinguishing difference in the distributions of the specific humidity near hurricane center between BG and BGM vortices is that the wet air extents to a much higher altitude in BGM than in BG. For instance, the 12 g kg^{-1} contour in BGM reaches a level (410 hPa) much higher than that in BG (580 hPa). In BGM, initial cloudwater and rainwater are also generated and their maxima are located in the upper and lower troposphere, respectively (Fig. 15b and c).

Compared with the initial vortex provided by large-scale analysis from the NCEP operational center, the vortices obtained by the BDA procedure(the experiments BG, BGSAT and BGM) have not only a central SLP and its location close to observations, but also very compact conceptually-consistent structures reflected in all model variables. Consistency of the initial vortex with model resolution, dynamics, and physics is guaranteed through the use of the forecast model as a strong constraint. Once a surface low is specified, changes in all the other model variables are obtained objectively. The question that needs to be answered is whether the initial conditions obtained by BDA will produce an improved prediction of Hurricane Felix. Results of several model predictions using the NCEP analysis and the initial conditions generated by the BDA initialization scheme are shown in the following section.

5 Improvements in the prediction of Hurricane Felix

A triply nested version of MM5 model (see Table 1) was integrated for 72 hours from four initial conditions of CTRL, BG, BGSAT and BGM, initializing at 00 UTC 16 August 1995. A significant improvement in the predicted track resulted from the use of the BG initial condition (Fig. 16). The 24-h forecast error decreased from 93 km (in CTRL) to 75 km (in BG). The smoothness of the track in experiment BG indicates that the initial adjustment of the vortex through the variational approach is well-adapted to the forecast model. By 48-h

the improvement in the storm track was even more significant. In the integration with the analyzed vortex (CTRL), the delay in the northeastward turning resulted in a 48-h forecast position error of about 170 km. In contrast, the simulated storm with the BG initial vortex followed the best track more closely, with the 48-h position error of about 76 km being almost similar to that of the previous 24 h. At 72 h the position error in CTRL continued to increase and was located about 193 km west-northwest of the actual storm position. The track error at 72 h of the BG forecast increased to 84 km, which is less than half of the position error in CTRL. The added satellite WVWV observations in BGSAT does not indicate much added value to the track prediction of Hurricane Felix. The forecast position errors were attributed to the excessive storm acceleration in the northwest direction. Thus, the improvements in the predicted storm position as a result of the proposed BDA scheme, facilitated the deceleration of the westward movement during the 48-h forecast prior to 00 UTC 19 August 1995.

The improvement of the forecast skill using the proposed BDA scheme is also reflected in the prediction of the intensity and structures of Hurricane Felix. Time series (at 6-h intervals) of the minimum SLP and maximum low-level winds determined at the lowest model level (σ = 0.995, approximately the 50-m height) are shown in Fig. 17. During the first 12 hours the observed storm experienced a gradual weakening, and leveling off in intensity thereafter. The observed central SLP value increased 6 hPa in first 12 hours. The predicted storm exhibited similar behavior and maintained a fairly stable level of intensity for the remaining period of the 72-h integration. Without the BDA scheme (CTRL), the difference in the SLP is more than 30 hPa weaker than the observed at initial time (t = 0 h). Such a large difference in the hurricane intensity is far too great to make up during the 72 hour of model integration in CTRL. The inclusion of the BDA scheme provided the model with a more vigorous storm at initial time, thus enabling it to simulate the level of intensity with remarkable agreement to the observed. It is indeed noteworthy to remark that the inclusion of satellite WVWV observations in BGSAT shows positive impact to the forecast intensity. The performance as measured by the averaged (over 3-day forecast period) position error, the deepening rate, and the maximum low-level wind in CTRL, BG, BGM, and BGSAT is summarized in Table 3. The mean error in intensity in BG is only 2.1 hPa compared with an average error of 25.9 hPa in CTRL. The error in the predicted SLP is reduced to 0.9 hPa with the inclusion

of cloudwater and rainwater variables in the prediction of moisture, and is further reduced to 0.4 hPa with the incorporation of satellite WVWV observations. The maximum low-level winds in BGSAT also show the best agreement with observations (Fig. 17b), with an averaged error of less than 0.1 m s^{-1} during the entire 72-h forecast period. In sharp contrast, the analyzed initial vortex when there is no BDA scheme introduced, the maximum low-level winds experience a marked decrease in strength in the first 6 h and only a gradual recovery and increase after 24 h. The averaged difference between the predicted and the best estimated maximum low-level winds in CTRL is as large 10.5 m s^{-1}, compared to about 1.1 m s^{-1} in BG. Inclusion of the microphysics scheme resulted in a slightly stronger low-level wind. The inclusion of satellite data is found to have a positive impact, albeit small, on the prediction of the storm's intensity.

Table 3: Mean errors of the 72-h forecasts

experiment	track (km)	central SLP (hPa)	maximum wind speed (m s^{-1})
CTRL	130 (52.7*)	25.9 (4.6)	-10.5 (5.3)
BG	64 (23.2)	2.1 (1.5)	-1.1 (2.3)
BGM	70 (26.7)	0.9 (1.9)	2.6 (2.3)
BGSAT	79 (24.2)	0.4 (1.2)	-0.11 (2.1)

*the root-mean-square errors

The close match of the predicted hurricane intensity with the observed values during the entire 72-h model integration is quite encouraging. The model's ability to produce and maintain the observed hurricane intensity right from the beginning of the model integration, without a spin-up period, demonstrates the advantage of using a full-physics forecast model as a strong constraint in the hurricane initialization procedure.

Figures 18a-d show the predicted flow field on 200 hPa and 850 hPa at 00 UTC 18 August 1995 (48-h forecasts) for both CTRL and BGSAT. We observe that the low sits in a upper-level westerly-northwesterly flow in CTRL, while in BGSAT the low is right below a center of upper-level cyclonic outflow with a wind maxima to its northeast side. The low

level winds near the surface low in BGSAT are not only much stronger than those in CTRL, but also assume a much more compact form surrounding the storm center. The maximum low-level wind in CTRL is 33.1 m s^{-1}, 180 km away from the storm center. In comparison, the maximum low-level wind in BGSAT reaches 42.3 s^{-1} and is located about 100 km to the east of the storm center.

Having seen the track, intensity, and flow features in the prediction of Hurricane Felix, we now examine the cloud and rainfall distributions. Figure 19 displays a visible satellite imagery at 1850 UTC 16 August 1995. As a comparison, Fig. 20 shows the domain C simulated hydrometeor fields described by vertically integrated cloudwater, ice, rainwater, and snow, which are the 18-h and 48-h prediction of BGSAT, as well as the corresponding vertical cross-sections cutting through the centers of the storm at both times. The simulated cloud distribution and the area of the storm at 18 UTC 16 August (Fig. 20a) conform to the satellite imagery well. Both the model and the observations show the development of organized spiral cloud bands with an echo-free eye in its central core. The model also simulates well the cellular convection at the outer edge and intense and organized clouds in the eyewall. The vertical distributions of the clouds (Figs. 20c and d) allow us to assess the capability of model prediction in simulating the inner-core structures of Felix. Maximum values of hydrometeor field appear at about 500 hPa northwest of the storm center and 700 hPa southeast of the storm center at 18 h and 450 hPa and 900 hPa at 48 h. The increase in the scale of the eye with height is small. The simulated Felix had about a 70 km wide eye at 18 h and 100 km wide eye at 48 h. The latter is very close to the aircraft radar report (about 92-130 km) during 17-19 August 1995. As a benchmark comparison, Fig. 21 shows the cloud distribution at 18 h for CTRL, similar to Fig. 20 a and c for BGSAT. We find that the cloud distribution in CTRL does not resemble what was observed (Fig. 19). The well-defined cellular convection at the outer edge of the storm, which is found in BGSAT (see Figs. 20a,c), is not observed. The two clouds maximum centers, one to the northeast side and the other to the southwest side, are too far away from the eye. A cross-section cutting through the center of the storm and reaching these two intense clouds (Fig. 21) does not reflect much of the vertical structures. The clouds exist with a very limited vertical extent (not exceeding 800 hPa).

The lack of cloud organization in CTRL possibly resulted from the problems of initial adjustment and false spin-up of the model vortex due to the lack of consistency between the analyzed initial vortex and model resolution and physics. This is reflected clearly in precipitation prediction. Fig. 22 shows the time evolution of the maximum amount of 6-h accumulated rainfall during the 72-h model integrations for the experiments CTRL and BGSAT. Significant rainfall does not start until 36 hours into the model integration in the control experiment CTRL. Before 36 hours, the 6-h accumulated rainfall is less than 83 mm. After 36-h of integration, the 6-h rainfall amount reaches 193 mm for the period of 36-42 h, 180 mm for 42-48 h and 204 mm for 48-54 h (figures omitted). In contrast, the model starting from the initial condition obtained after assimilation of the bogused surface low and satellite WVWV observations (BGSAT) does not suffer from such a serious precipitation spin-up problem. The initial 6-h rainfall reaches a maximum value of 308 mm. The maximum 6-h rainfall in BGSAT is 228 mm for the period of 36-42 h, 211 mm for 42-48 h and 220 mm for 48-54 h (figures omitted). Although the amount of the precipitation in CTRL after 36 h comes close to that in BGSAT, regions of maximum precipitation in BGSAT are located much closer to the hurricane center compared with those in CTRL. Figure 23, for example, shows the distribution of the 6-h accumulated rainfall during 36-42 h for CTRL and BGSAT. The precipitation pattern in BGSAT is closer to the hurricane eye and more circularly shaped around the hurricane center than that in CTRL.

The large differences in precipitation between CTRL and BGSAT during the initial 36 h of model integration could result in a significant difference in the amount of latent heat release, which is in turn attributable to the enhanced low-level convergence of mass and moisture and upper-level divergence of mass. These and the coherent structures in the BDA-derived initial vortex contributed significantly to the improvement in the prediction of Hurricane Felix.

6 Summary and conclusions

The purpose of this paper is to present a BDA scheme for hurricane initialization. The dynamic and thermodynamic structures of the initial vortex obtained by the BDA procedure

are examined, and the improvements to the prediction of the hurricane track, the intensity change, and the structural features are demonstrated. The proposed BDA scheme requires minimum observational information involving the determination of the numerical values of a few parameters such as the size, the location, and the central value of the specified surface low. The hurricane prediction model serves as a strong constraint to spin-up other fields not readily observed. Satellite and radar data observations can be combined with the bogus information to generate a more realistic tropical cyclone.

The BDA scheme has been tested on the initialization and the 72-h prediction of Hurricane Felix (1995) during its mature stage. We show that the specification of the surface low alone is quite effective in generating a consistent 3-dimensional structure of the initial vortex without the need of an "artificial" specification of other meteorological fields. By assimilating the surface pressure data representing the specified surface low in a 4-dimensional space with the hurricane forecast model and its adjoint model serving to carry information forward and backward in time, a model state can be generated which contains a surface low with realistic size and intensity, the anticyclonic outflow in the upper-level and the cyclonic inflow in the lower level, a strong upward motion around the vortex eye, and a warm and moist core near the center of the initial vortex. Since the initial model state obtained by BDA was well-adapted to the forecast model, dramatic improvements are observed in the track and intensity forecast as well as the description of the inner structures of the predicted storm during a 3-day forecasting period. The model is able to generate large amounts of precipitation during the first few hours of numerical simulation, avoiding the spin-up problem associated with the traditional hurricane bogusing scheme. The track error is also reduced by half. Due to the use of a short time window, the proposed scheme, though carried out in a 4-dimensional space, is considered to be operationally feasible.

Application of the proposed scheme to another hurricane simulation, Hurricane Fran, also shows similar improvements to the initial conditions (Xiao and Zou, 1998). Tests of this scheme with various values of the size of the surface low have produced very similar results, showing a minimum sensitivity to the subjectively determined radius of the surface low. Sensitivity of the BDA results to the formulation of the surface pressure field based on a few observed or estimated parameters (other models instead of the Fujita's formula) and

the performance of the BDA scheme on a weak initial vortex are being conducted and will be presented in our future work. Given the current advances in numerical forecast models and large-scale analysis, our results suggest that it may be possible to predict the track, intensity, and inner-core structures of hurricanes reasonably well with new observations (such as satellite-derived WVWVs, ozone data and/or radar reflectivities and radial winds) and a minimum amount of added (or "targeted") observational information such as a number of surface pressure observations within the storm region.

Acknowledgment. The authors would like to thank R. Rotunno and S. Low-Nam, and the anonymous reviewers for their useful suggestions concerning this paper. The authors would also like to thank Chris Velden at the University of Wisconsin for providing us the satellite-derived water vapor wind vector data associated with Hurricane Felix. This research is partially supported by AFOSR through project number F4920-96-C-0020.

7 REFERENCES

Bender, M. A., R. J. Ross, R. E. Tuleya, and Y. Kurihara, 1993: Improvements in tropical cyclone track and intensity forecasts using the GFDL initialization system. *Mon. Wea. Rev.* **121**, 2046-2061.

Courtier, P., J.-N. Thépaut, and A. Hollingsworth, 1994: A strategy for operational implementation of 4D-Var, using an incremental approach. *Q. J. R. Meteorol. Soc.*, **140**, 1367-1387.

Courtier, P., E. Andersson, W. Heckley, J. Pailleux, D. Vasiljević, M. Hamrud, A. Hollingsworth, F. Rabier and M. Fisher, 1998: The ECMWF implementation of three-dimensional variational assimilation (3D-Var). I: Formulation, *Q. J. R. Meteorol. Soc.*, **124**, 1783-1808.

Dudhia, J., 1993: A nonhydrostatic version of the Penn State-NCAR mesoscale model: Validation tests and simulation of an Atlantic cyclone and cold front. *Mon. Wea. Rev.* **121**, 1493-1513.

Dvorak, V., 1995: Tropical clouds and cloud systems observed in satellite imagery: Tropical cyclones. Workbook Vol. 2. [Available from NOAA/NESDIS, 5200 Auth Rd., Washington, DC 20233.]

Fujita, T., 1952: Pressure distribution within a typhoon. *Geophys. Mag.*, **23**, 437-451.

Grell, G. A., J. Dudhia, and D. R. Stauffer, 1994: A description of the fifth-generation Penn State/NCAR mesoscale model (MM5). *NCAR Technical Note*, NCAR/TN-398 + STR, National Center for Atmospheric Research, Boulder, CO, 138 pp.

Krishnamurti, T. N., S. K. Roy Bhowmik, D. Oosterhof, and G. Rohaly, 1995: Mesoscale signatures within the tropics generated by physical initialization. *Mon. Wea. Rev.*, **123**, 2771-2790.

Krishnamurti, T. N., D. Oosterhof, and N. Dignon, 1989: Hurricane prediction with a high resolution global model. *Mon. Wea. Rev.*, **117**, 631-669.

Krishnamurti, T. N., J. Xue, H. S. Bedi, K. Ingles, and D. Oosterhof, 1991: Physical initialization for numerical weather prediction over tropics. *Tellus*, **43AB**, 53-81.

Kurihara, Y., M. A. Bender and R. J. Ross, 1993: An initialization scheme of hurricane models by vortex specification. *Mon. Wea. Rev.*, **121**, 2030-2045.

Kurihara, Y., R. E. Tuleya, and M. A. Bender, 1998: The GFDL hurricane prediction system and its performance in the 1995 hurricane season. *Mon. Wea. Rev.*, **126**, 1306-1322.

Kurihara, Y., R. E. Tuleya, and R. J. Ross, 1990: Prediction experiments of Hurricane Gloria, 1985, using a multiply-nested movable mesh model. *Mon. Wea. Rev.*, **118**, 2185-2198.

Liu, Y., D.-L. Zhang, and M. K. Yau, 1997: A multiscale numerical study of Hurricane Andrew (1992). Part I: Explicit simulation and verification. *Mon. Wea. Rev.*, **125**, 3073-3093.

Lord, S. J., 1991: A bogusing system for vortex circulations in the National Meteorological Center global forecast model. The 19th Conference on Hurricanes and Tropical Meteorology, American Meteorological society, 6-10 May, 1991, Miami, Florida. 328-330.

Navon, I. M., X. Zou, J. Derber, and J. Sela, Variational data assimilation with an adiabatic version of the NMC spectral model, *Mon. Wea. Rev., 120*, 1433-1446, 1992.

Parrish, D. F., and J. C. Derber, 1992: The National Meteorological Center's spectral statistical-interpolation analysis system, *Mon. Wea. Rev.*, **120**, 1747-1763.

Trinh, Van Thu and T. N. Krishnamurti, 1992: Vortex initialization for Typhoon track prediction. *Meteorol. Atmos. Phys.*, **47** 117-126.

Velden, S. V., C. M. Hayden, S. J. Nieman, W. P. Menzel, S. Wanzong, and J. S. Goerss, 1997: Upper-tropospheric winds derived from geostationary satellite water vapor observations. *Bull. Amer. Met. Soc.*, **78**, 173-195.

Willoughby, H. E., 1995: Mature structure and evolution. Global Perspectives on Tropical Cyclones. World Meteorological Organization Technical Document. WMO/TD-No. 693. Report No. TCP-38. 21-62.

Xiao, Q., and X. Zou, 1998: Variational bogus and numerical simulation of Hurricane Fran (1996). The Eighth PSU/NCAR Mesoscale Model User's Workshop, 98-102.

Zou, X., I. M. Navon, and F. X. Le Dimet, 1992: Incomplete Observations and Control of Gravity Waves in Variational Data Assimilation, *Tellus*, **44A**, 273-296.

Zou, X., I. M. Navon and J. Sela, 1993: Control of Gravity Oscillations in Variational Data Assimilation. *Mon. Wea. Rev.*, **121**, 272-289.

Zou, X., Y.-H. Kuo, and Y.-R. Guo, 1995: Assimilation of atmospheric Radio Refractivity Using a Nonhydrostatic Adjoint Model. *Mon. Wea. Rev., 123*, 2229-2249, 1995.

Zou, X., F. Vandenberghe, M. Pondeca, and Y.-H. Kuo, 1997: Introduction to Adjoint Techniques and the MM5 Adjoint Modeling System, *NCAR Technical Note*, NCAR/TN-435 - STR, National Center for Atmospheric Research, Boulder, CO, 110pp.

CAPTIONS

Figure 1: Observed track (best track determined by the National Hurricane Center) of Hurricane Felix during the period from 00 UTC 12 August 1995 to 00 UTC 22 August 1995. The large dots indicate the position of the storm at 00 UTC and the x's indicate the 06, 12 and 18 UTC storm positions. The storm's minimum SLP (hPa) and maximum low-level wind (m s^{-1}) are shown at 00 UTC each day. The initial time for the numerical simulations of Hurricane Felix in this study is 00 UTC 16 August 1995.

Figure 2: Geographical locations of the three model domains (see Table 1 for more detailed information).

Figure 3: Grid points where values of the bogus surface pressure (thin solid) are assimilated into the MM5 forecast model. The minimum value of the specified surface low is 963 hPa. Contour interval is 4 hPa. The SLP from the NCEP analysis outside the specified surface low is shown as thick solid lines. Line AB indicates the position for the cross-sections of Figures 9 and 15. Line CD is the position for the cross-sections of Figure 13.

Figure 4: Satellite-derived (GOES-8) water vapor wind vectors (6.7-μm channel) with assigned heights (a) between 150-250 hPa and (b) below 500 hPa at 00 UTC 16 August 1995. The wind vectors, interpolated from the NCEP analysis at 00 UTC 16 August 1995 to the satellite observational locations, are plotted in (c) and (d), corresponding to (a) and (b) respectively. A full bar represents 5 m s^{-1}.

Figure 5: The adjustments in the zonal wind (Du) of the initial condition resulted from the assimilation of a specified surface low (the experiment BG). (a) 200 hPa, (b) 300 hPa, (c) 500 hPa and (d) 850 hPa. The contour interval is 2 m s^{-1} for (a) and (d) and 1 m s^{-1} for (b) and (c).

Figure 6: Same as Fig. 5, except for the meridional wind component (Dv).

Figure 7: The streamlines, the SLP (thin-dashed line) and the wind speed (thick-solid line) for (a) CTRL at 200 hPa, (b) BG at 200 hPa, (c) CTRL at 850 hPa and (d) BG at 850 hPa. The contour intervals for the SLP and wind speed are 2 hPa and 5 m s^{-1}, respectively.

Figure 8: The adjustments in the initial condition of the (a) temperature at 850 hPa, (b) SLP, (c) specific humidity at 850 hPa, and (d) vertical velocity at 850 hPa for the experiment BG. Contour intervals for the temperature, SLP, specific humidity and vertical velocity are 1°C, 3 hPa, 1 g kg^{-1} and 10 cm s^{-1}, respectively.

Figure 9: Cross-sections of the (a) temperature and (b) specific humidity at the initial time for the experiment BG. Contour intervals for the temperature and specific humidity are 4°C and 2 g kg^{-1}, respectively. Line AB is indicated in Figure 3 and the distance between A and B is 900 km.

Figure 10: The root-mean-square (rms) differences of the adjustment occurred at each iteration during the minimization procedure of the experiment BG. (a) $D^{(k)}u$, (b) $D^{(k)}v$, (c) $D^{(k)}w$, (d) $D^{(k)}p'$, (e) $D^{(k)}T$, and (f) $D^{(k)}q$, where the superscript k is the number of iterations. Contour intervals for $D^{(k)}u$, $D^{(k)}v$, $D^{(k)}w$, $D^{(k)}p'$, $D^{(k)}T$, and $D^{(k)}q$ are 0.1 m s^{-1}, 0.1 m s^{-1}, 1 cm s^{-1}, 0.3 hPa, 0.05°C, and 0.05 g kg^{-1}, respectively.

Figure 11: The adjustment in the initial condition of zonal wind at 850 hPa between (a) the second and the first iterations and (b) the fifth and the fourth iterations. Figures (c) and (d) are the same as (a) and (b) except for the adjustment in the initial condition of temperature at 850 hPa. The isopleths for (a) and (b) are ± 0.1, ± 0.5, ± 1.0, ± 2.0, ± 3.0, ± 4.0, ± 5.0, ± 6.0 m s^{-1}. For (c) and (d), the negative isopleth has an interval of 0.1 ^oC and the positive isopleths are 0.1°C, 0.5°C, and those with values larger than 0.5 ^oC having an interval of 0.5 °C.

Figure 12: Variation of the maximum values of the half-hour accumulated rainfall (unit: cm) with respect to the number of iterations.

Figure 13: Cross-sections of the vertical velocity along the line CD (see Figure 3) at the initial time for the experiments of (a) BG and (b) BGSAT. The contour interval is -10 cm s^{-1} for descent and 40 cm s^{-1} for ascent.

Figure 14: The cloud and rainfall distribution for the experiment BGM. (a) Vertically integrated cloudwater and rainwater at initial time (unit: mm), and (b) the initial half-hour accumulated rainfall (unit: cm).

Figure 15: Cross-sections of the initial condition of (a) specific humidity (q), (b) cloudwater (q_c) and (c) rainwater (q_r) for the experiment BGM. Line AB is indicated in Figure 3 and the distance between A and B is 900 km. Contour intervals for q, q_c and q_r are 2 k kg^{-1}, 0.5 g kg^{-1} and 0.5 g kg^{-1}, respectively.

Figure 16: The predicted hurricane tracks from 00 UTC 16 to 00 UTC 19 August 1995 for CTRL (circle), BG (cross), BGM (triangle) and BGSAT (star). The observed best track (dot) is also shown. The track positions are shown at 6-h interval.

Figure 17: Variation of the (a) minimum SLP (hPa) and (b) maximum low-level winds (m s^{-1}) (determined at the lowest model level σ=0.995, about 50-m high) with respect to the forecast time at a 6-hour interval. The symbols are the same as in Fig. 16.

Figure 18: The 48-h prediction of the SLP (thin dashed line), as well as the upper and low-level flows and the wind speed (thick solid line). a) CTRL at 200 hPa, (b) BGSAT at 200 hPa, (c) CTRL at 850 hPa, (d) BGSAT at 850 hPa. Contour intervals for the SLP and wind speed are 2 hPa and 5 m s^{-1}, respectively.

Figure 19: Visible satellite imagery at 1850 UTC 16 August 1995.

Figure 20: Vertically integrated cloudwater, rainwater and snow (mm) at (a) 18-h and (b) 48-h in the experiment BGSAT, as well as the vertical cross-sections of the total cloudwater, rainwater and snow (mm) at (c) 18-h along the line EF in (a) and at (d) 48-h along the line GH in (b).

Figure 21: Same as Figs. 20a and c except for the CTRL experiment. The cross-section of the total cloudwater, rainwater and snow (mm) is along the line IJ in Fig. 21(a).

Figure 22: Time series of the maximum value of the 6-h rainfall (mm) during the 72-h model integrations for the experiments CTRL (dashed line) and BGSAT (solid line).

Figure 23: 6-h accumulated rainfall during the time period from 36 h to 42 h in (a) CTRL and (b) BGSAT (unit: mm). The hurricane positions indicated are the 6-h average positions predicted in each experiment.

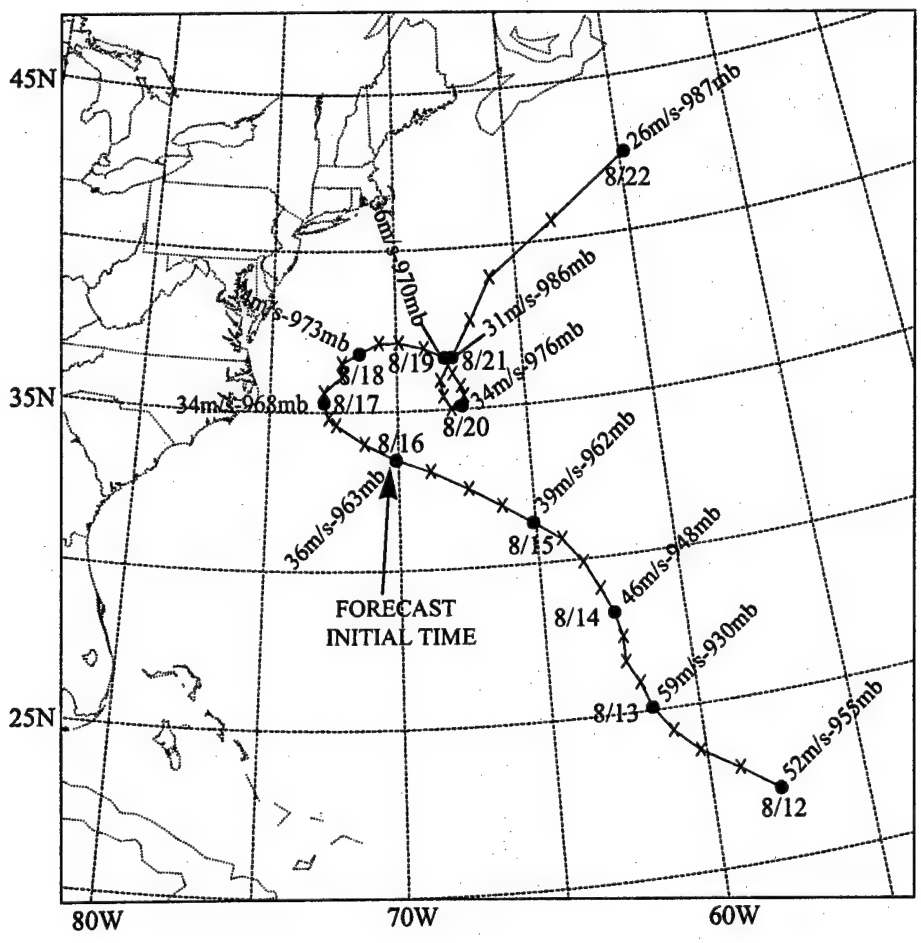
45N
35N
25N
80W
70W
60W
26m/s-987mb
8/22
36m/s-970mb
31m/s-986mb
40m/s-973mb
8/18
8/19
8/21
34m/s-976mb
34m/s-968mb
8/17
8/20
8/16
39m/s-962mb
36m/s-963mb
8/15
46m/s-948mb
FORECAST
INITIAL TIME
8/14
59m/s-930mb
8/13
52m/s-955mb
8/12

Fig.1

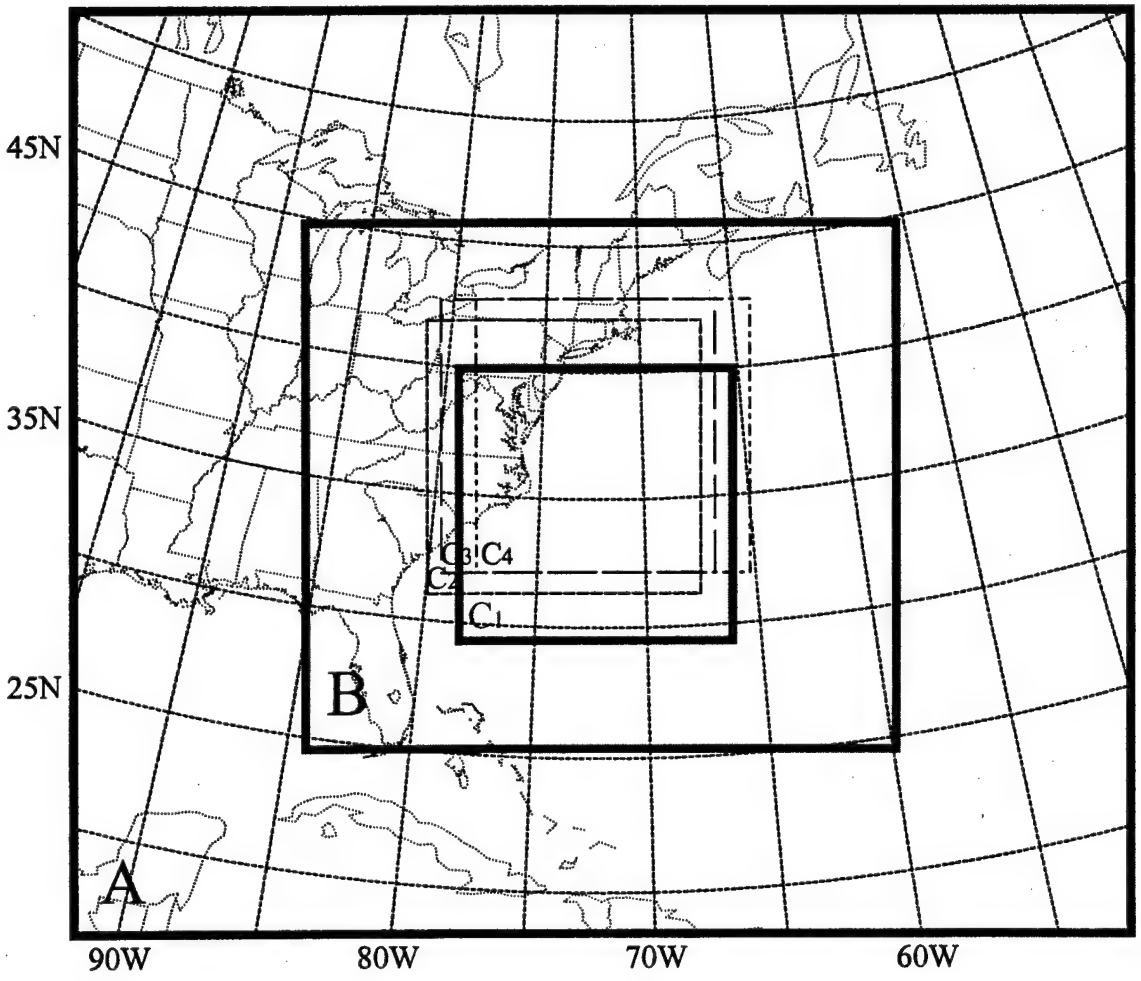

Fig.2

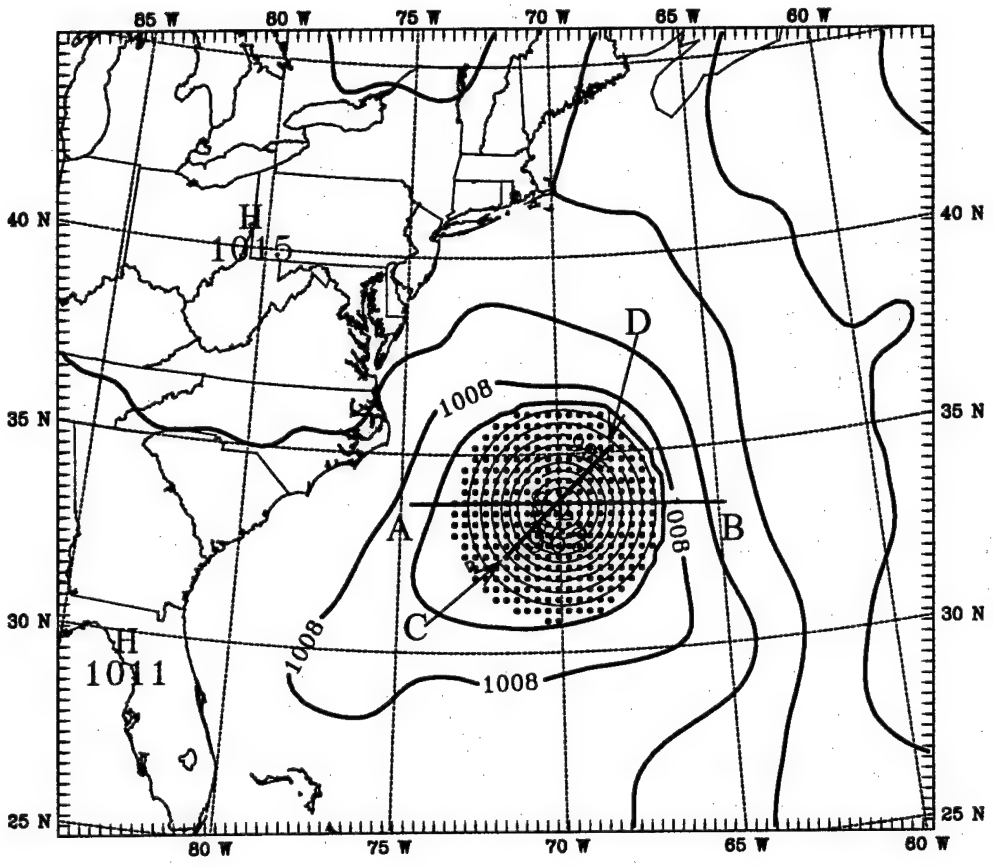
85 W
80 W
75 W
70 W
65 W
60 W
40 N
35 N
30 N
25 N
H
1015
H
1011
1008
1008
1008
1008
A
B
C
D

Fig.3

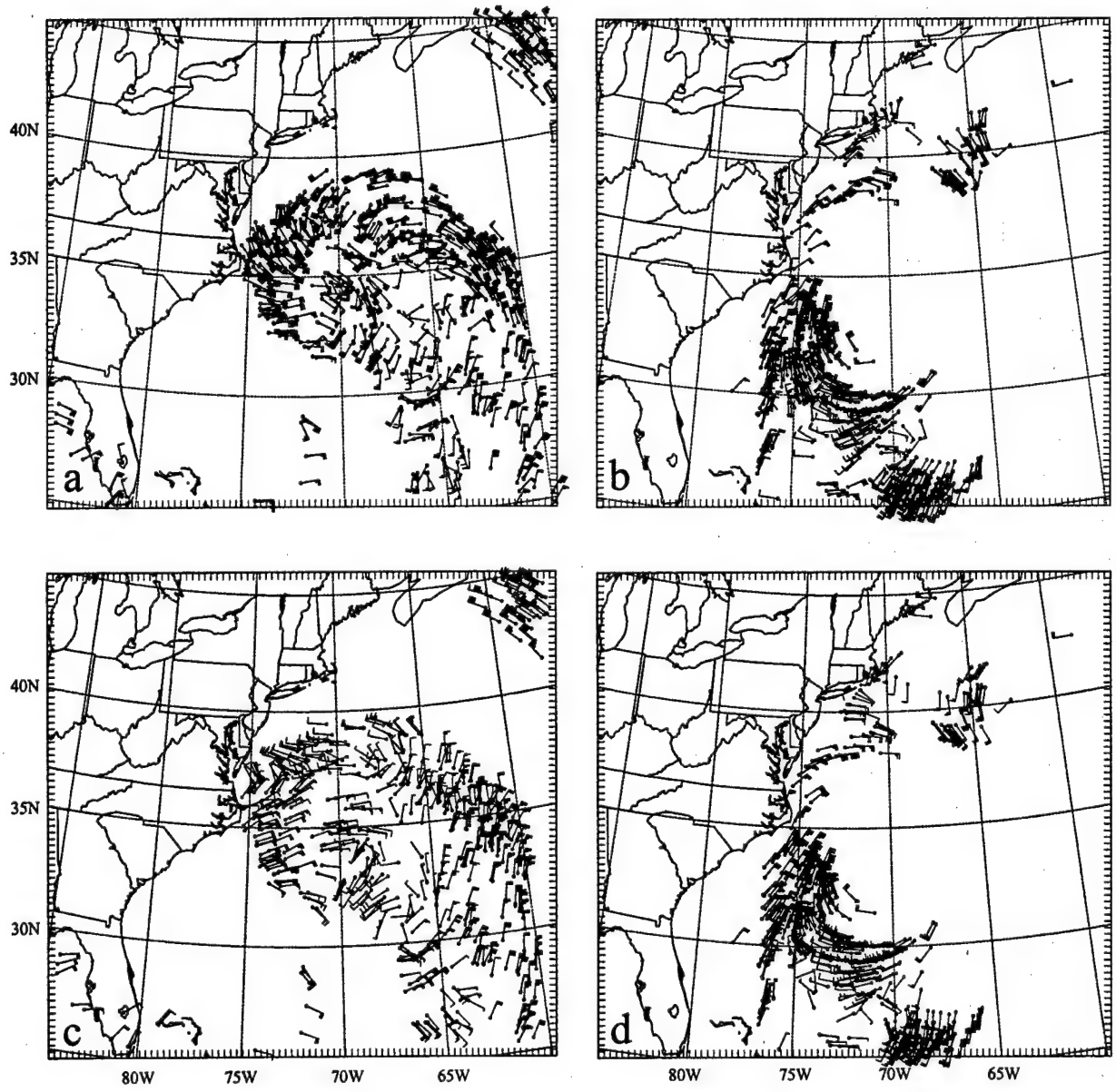

Fig.4

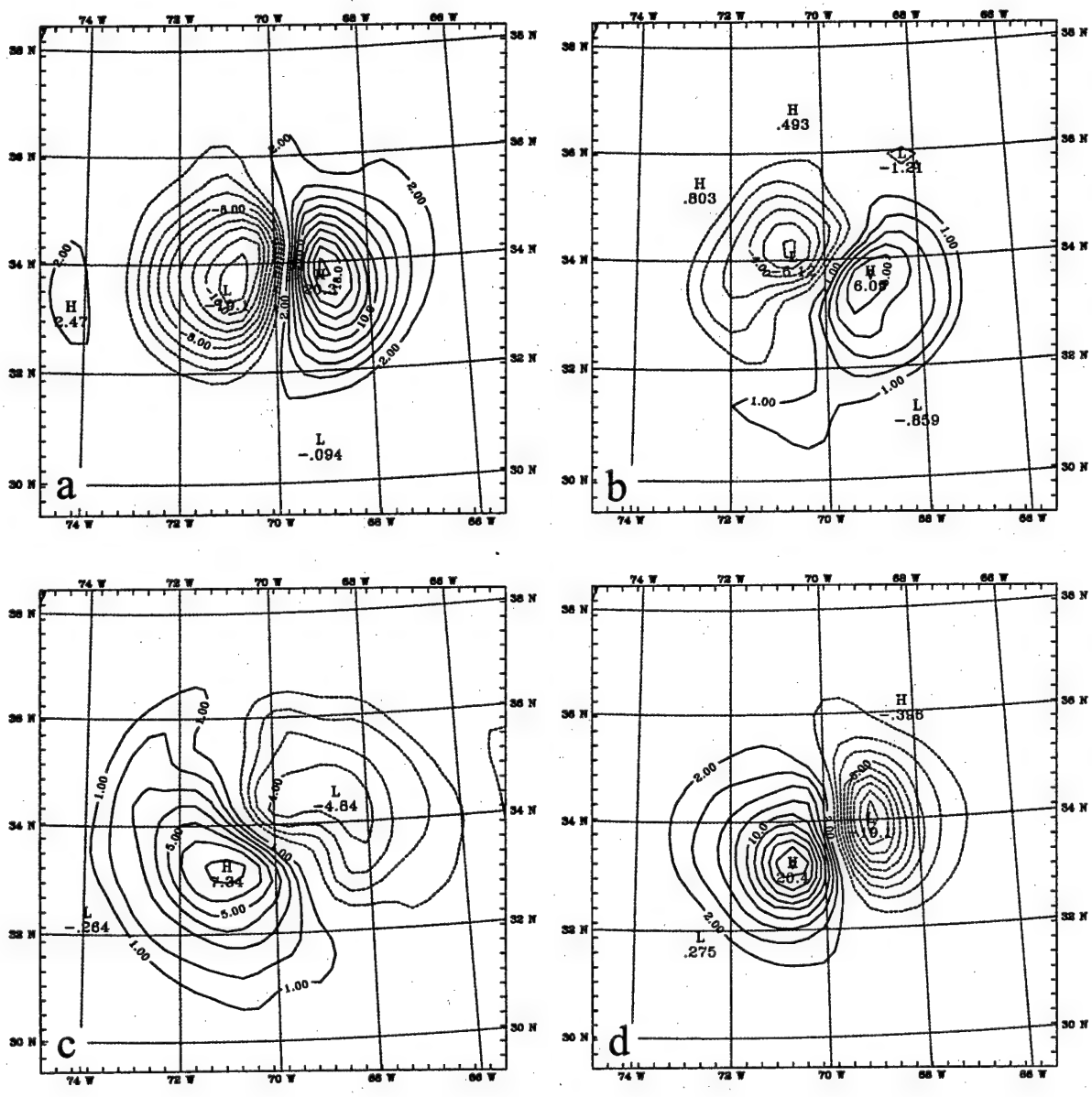
74 W
72 W
70 W
68 W
66 W
38 N
36 N
34 N
32 N
30 N
a
H
2.47
L
-.094
b
H
.493
H
.803
L
-1.21
L
-.859
6.09
c
H
7.34
L
-4.84
L
-.264
d
H
-.396
H
20.4
L
.275

Fig.5

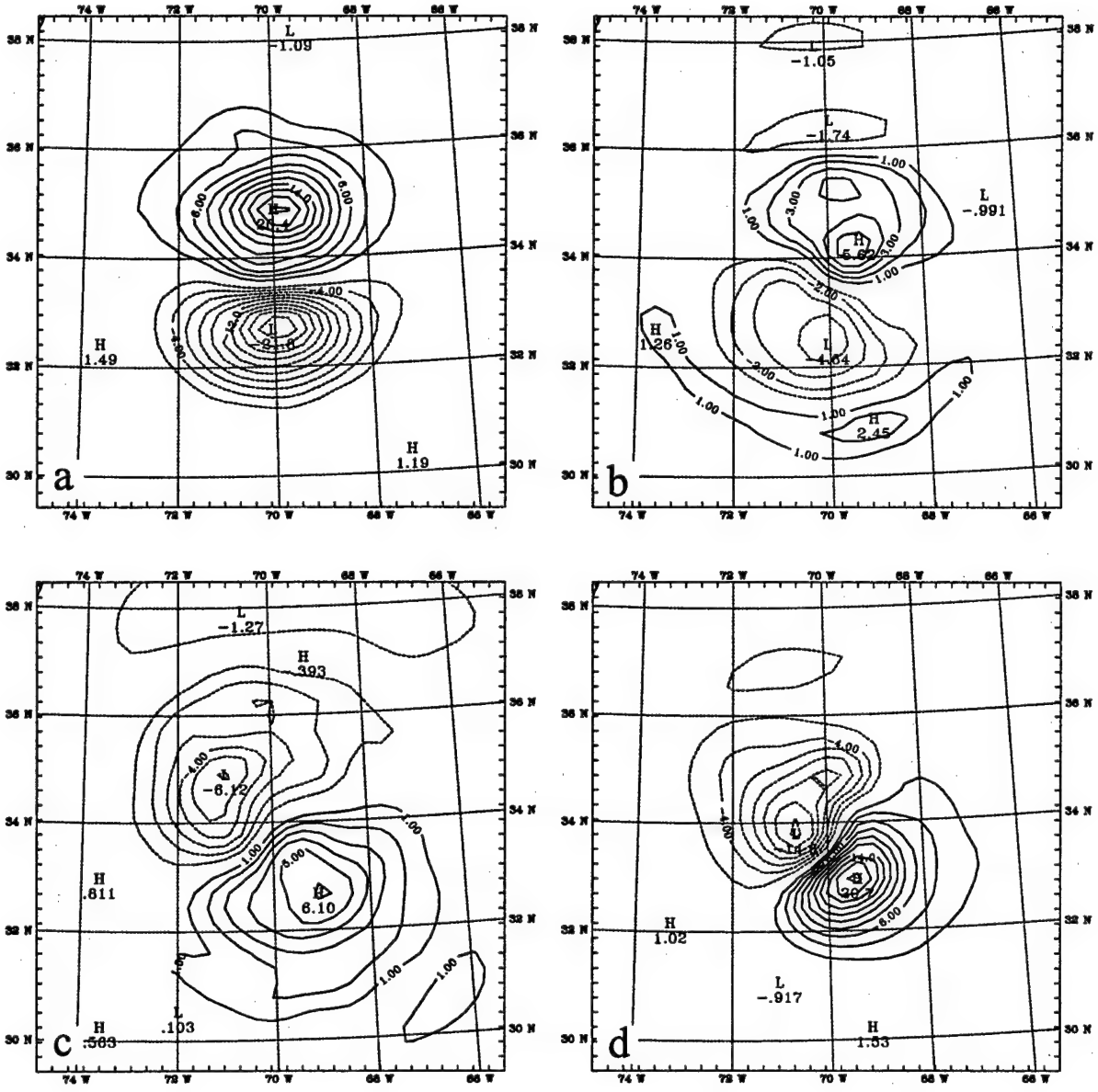
a
b
c
d
L
-1.09
H
1.49
H
1.19
L
-1.05
L
-1.74
L
-.991
H
1.26
L
4.64
H
2.45
L
-1.27
H
393
-6.12
H
.811
6.10
L
.103
H
.563
H
1.02
L
-.917
H
1.53

Fig.6

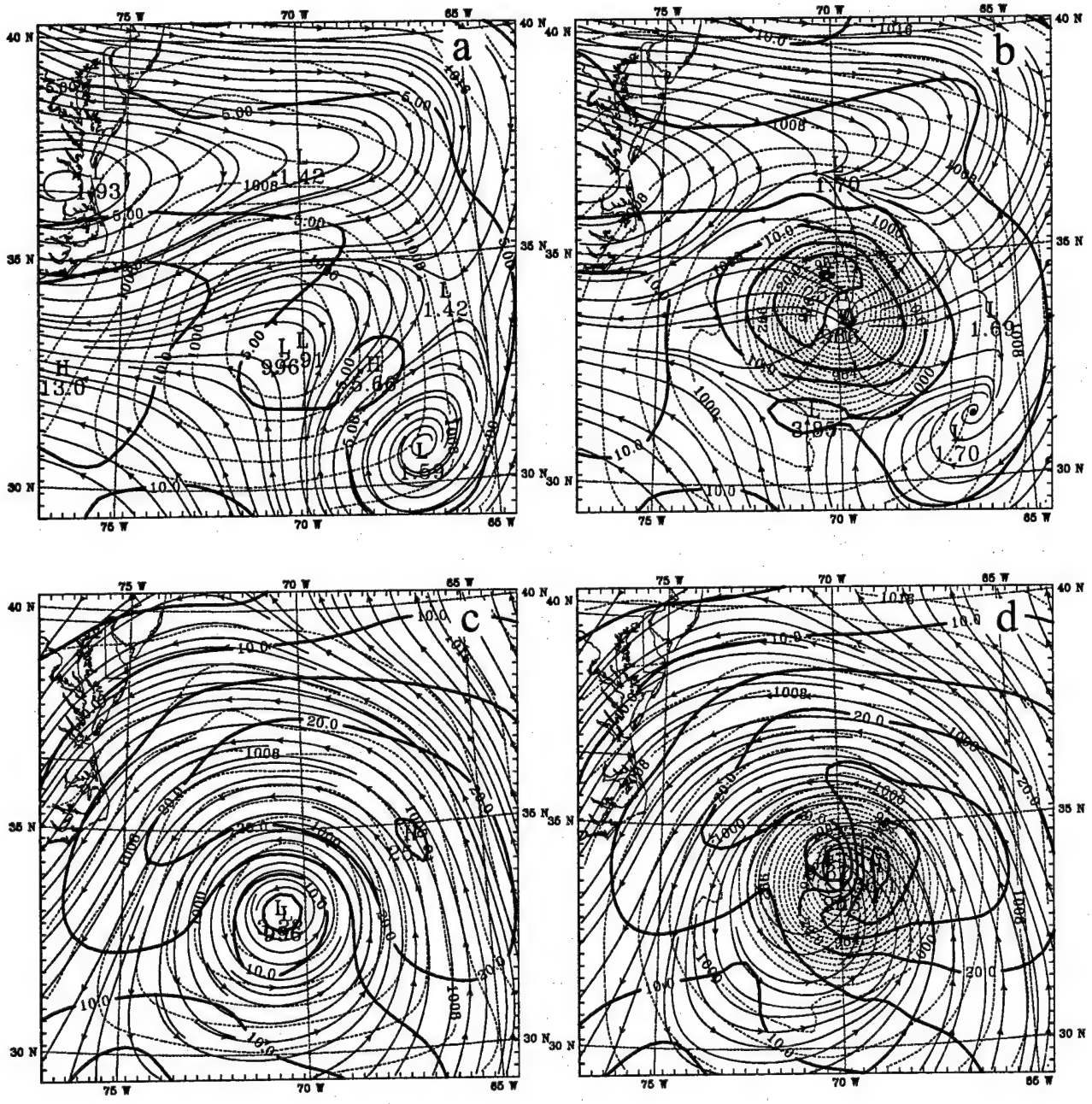

Fig.7

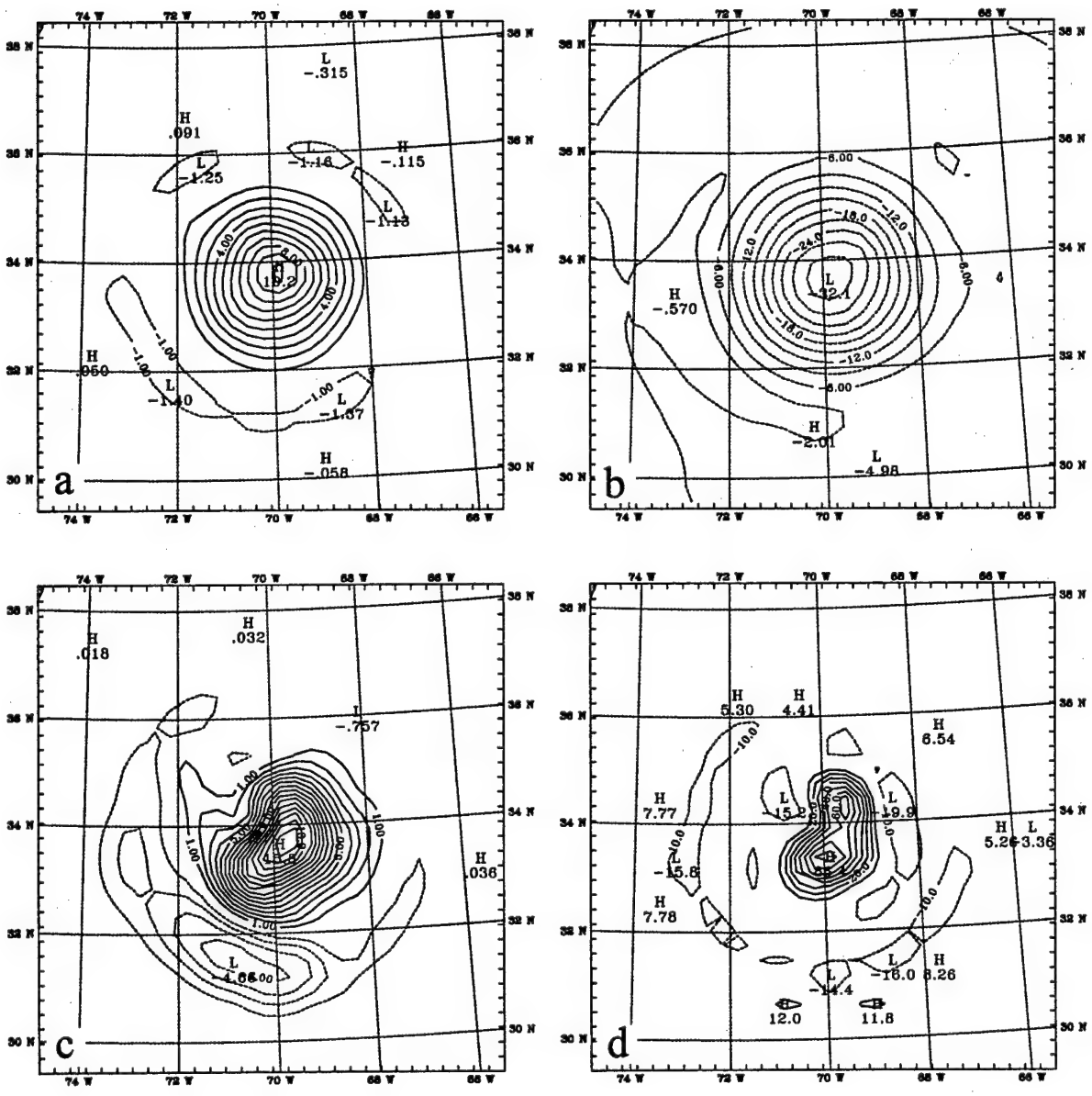

Fig.8

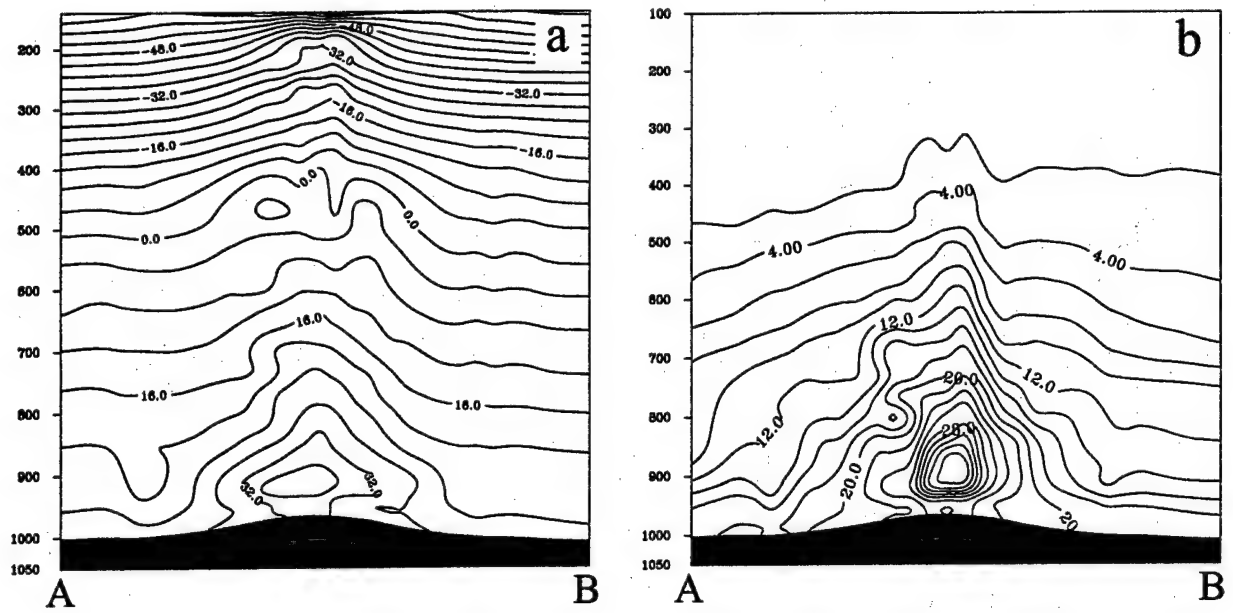

Fig.9

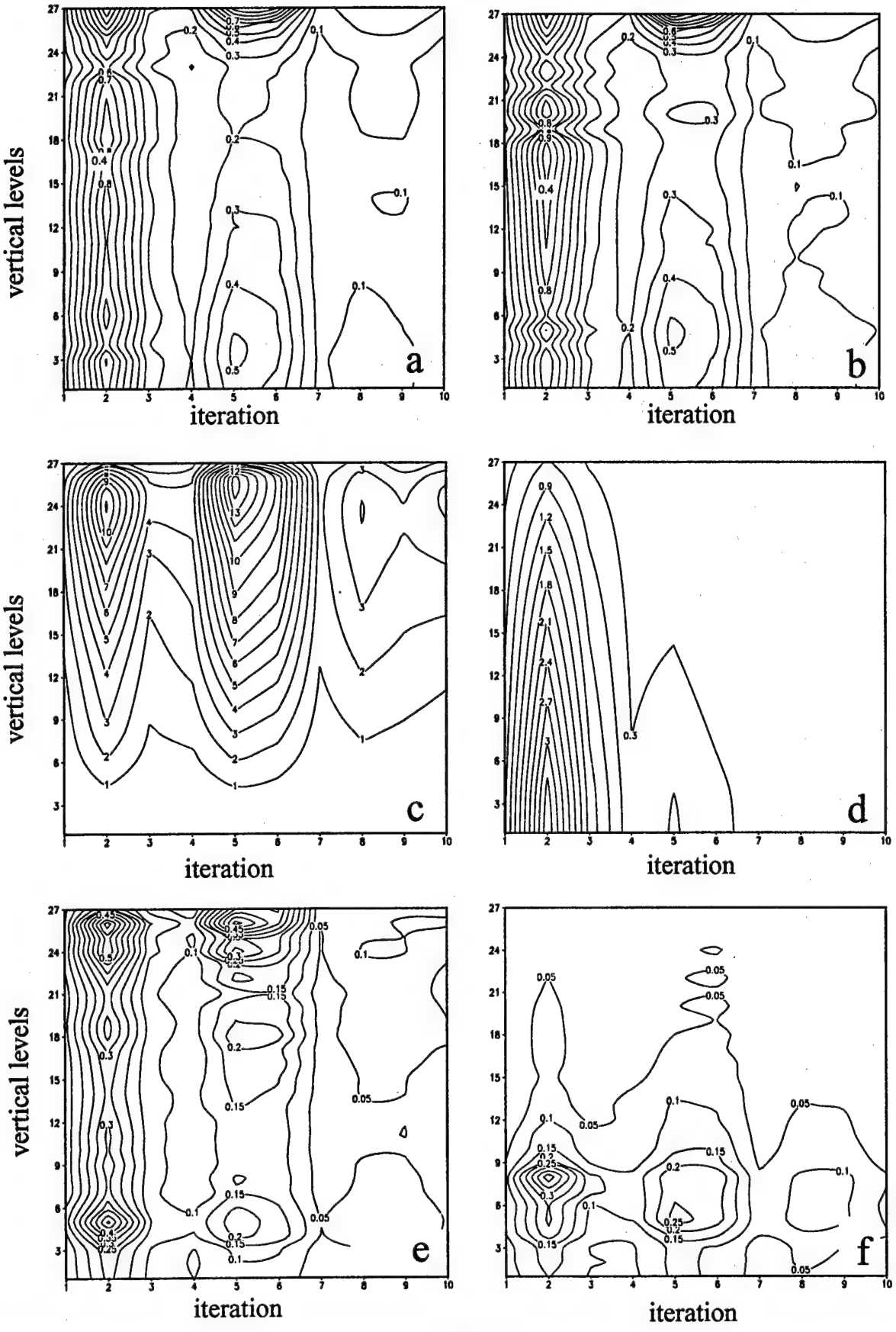

Fig.10

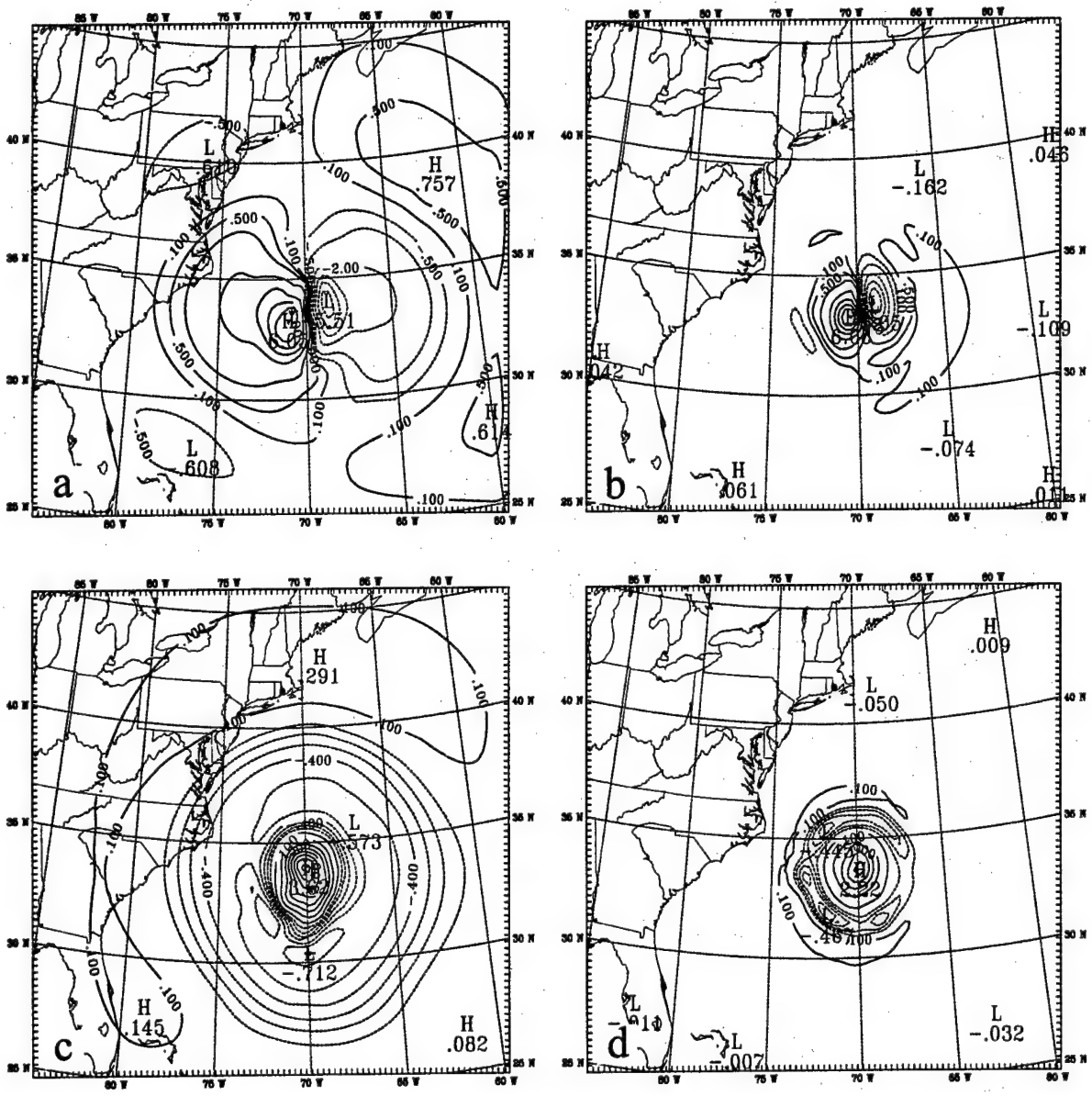
a
b
c
d
H
.757
L
.608
H
.614
L
-.162
H
.042
L
-.109
L
-.074
H
.291
L
.573
H
.145
H
.082
H
.009
L
-.050
L
-.032

Fig.11

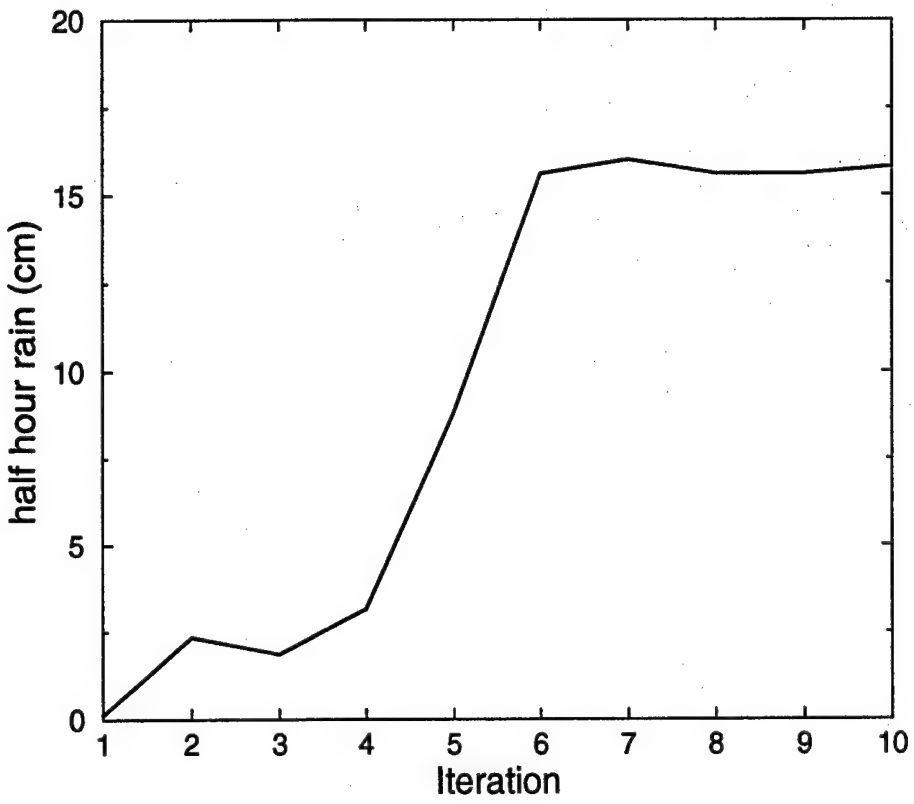

Fig. 12

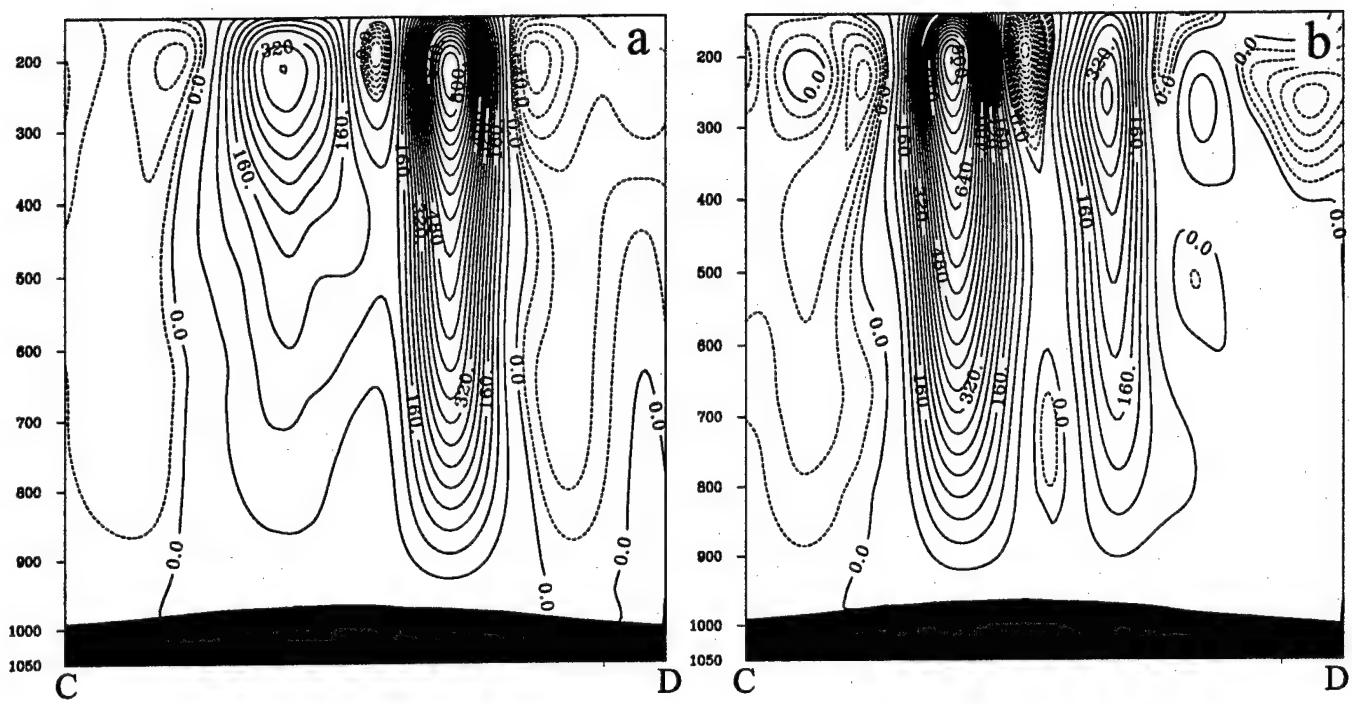

Fig. 13

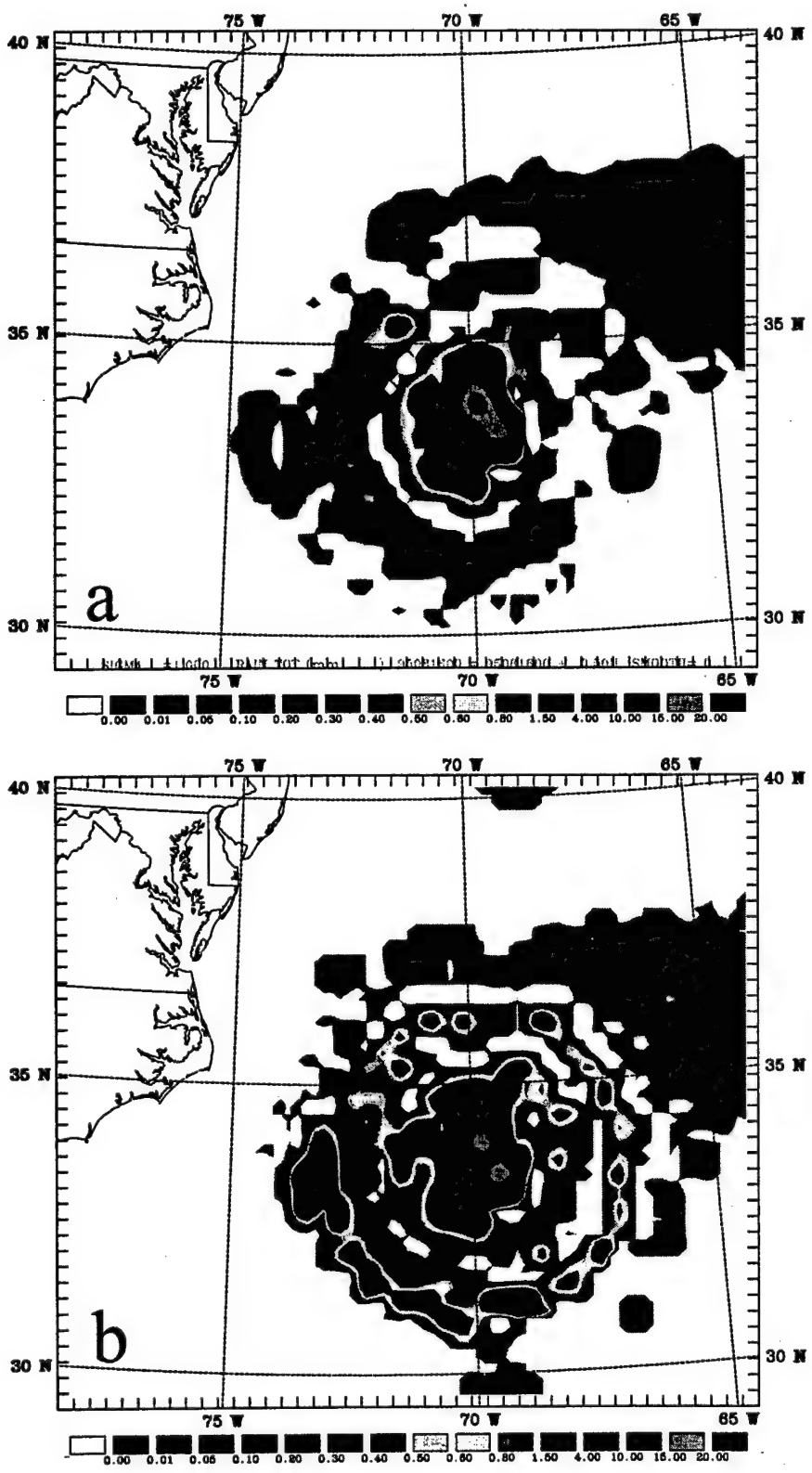
75 W
70 W
65 W
40 N
35 N
30 N
a
0.00 0.01 0.05 0.10 0.20 0.30 0.40 0.50 0.60 0.80 1.50 4.00 10.00 15.00 20.00
b

Fig. 14

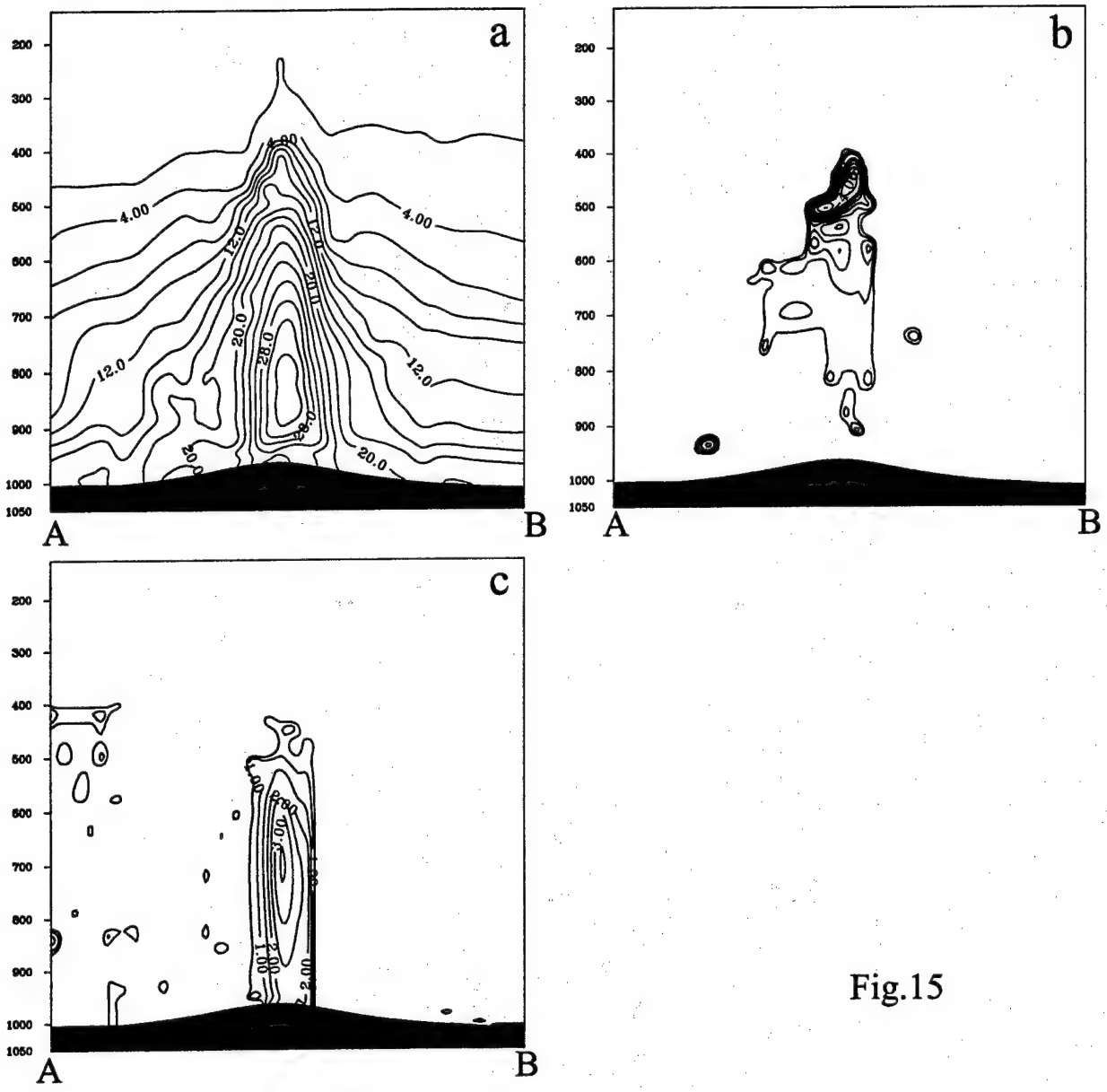

Fig.15

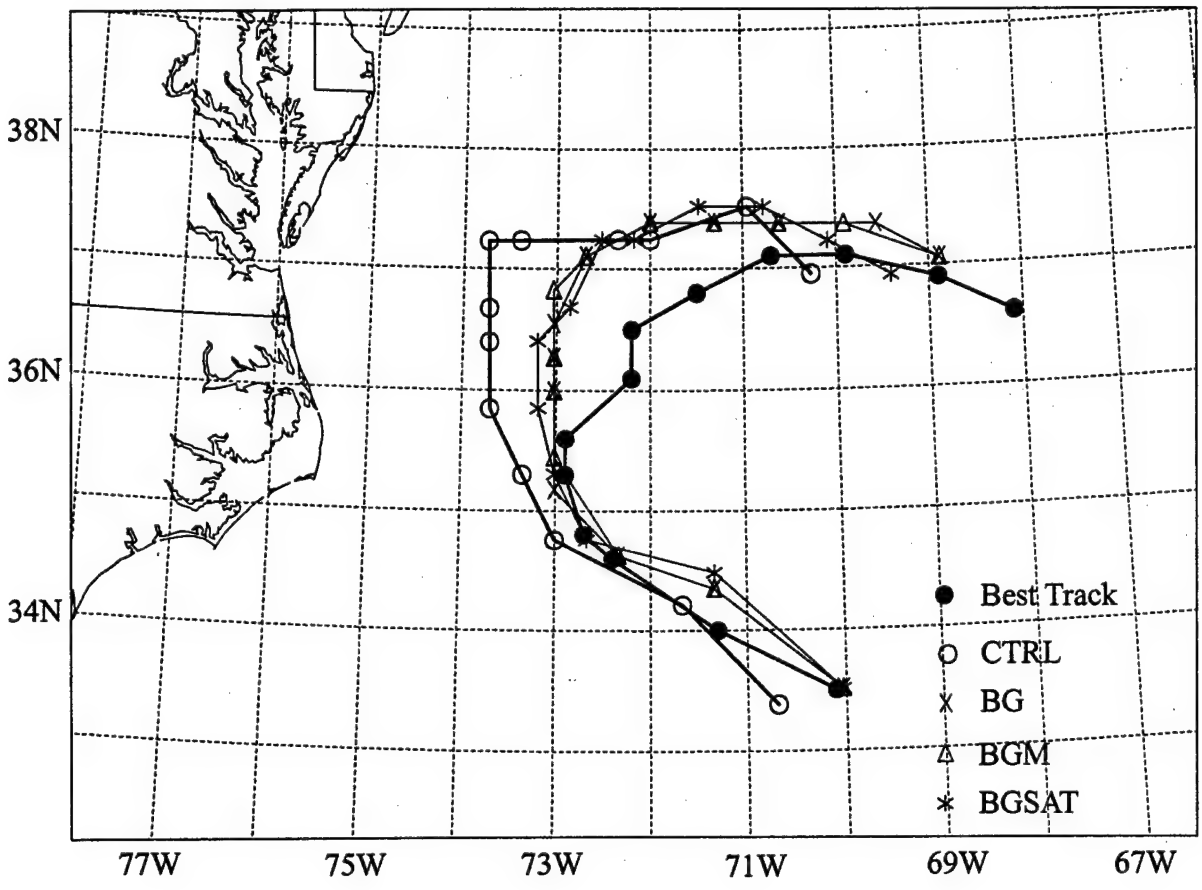
38N
36N
34N
77W
75W
73W
71W
69W
67W
Best Track
CTRL
BG
BGM
BGSAT

Fig. 16

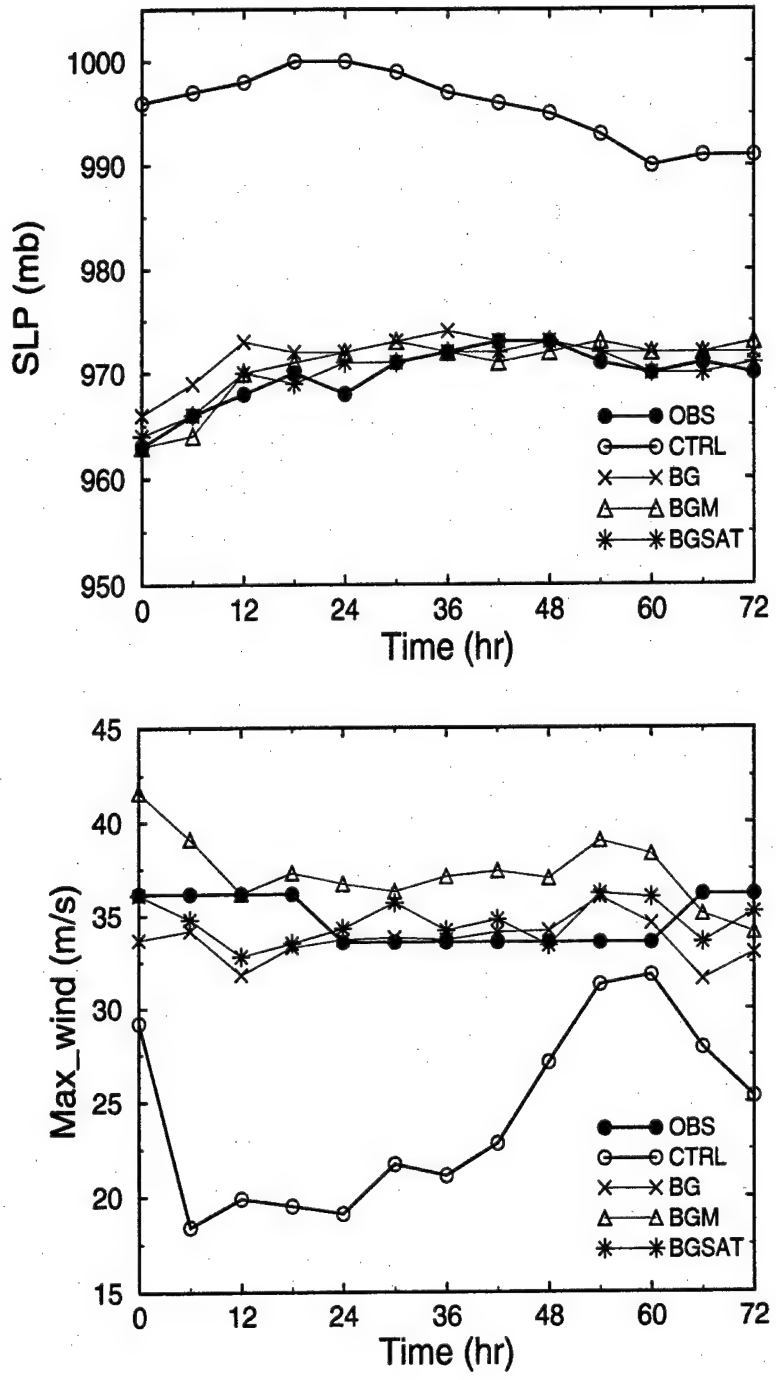
SLP (mb)
1000
990
980
970
960
950
0
12
24
36
48
60
72
Time (hr)
OBS
CTRL
BG
BGM
BGSAT
Max_wind (m/s)
45
40
35
30
25
20
15
0
12
24
36
48
60
72
Time (hr)
OBS
CTRL
BG
BGM
BGSAT

Fig. 17

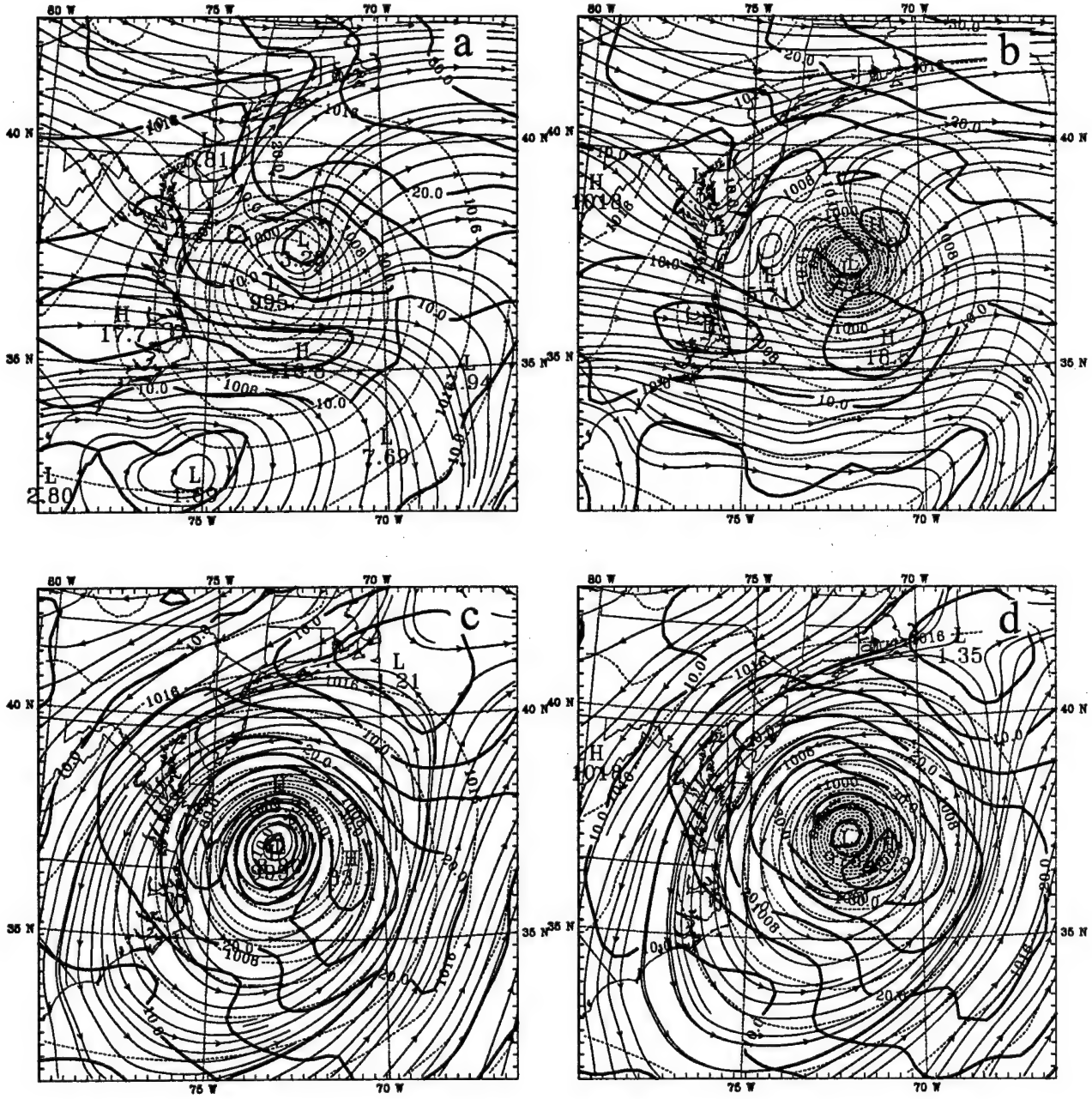

Fig.18

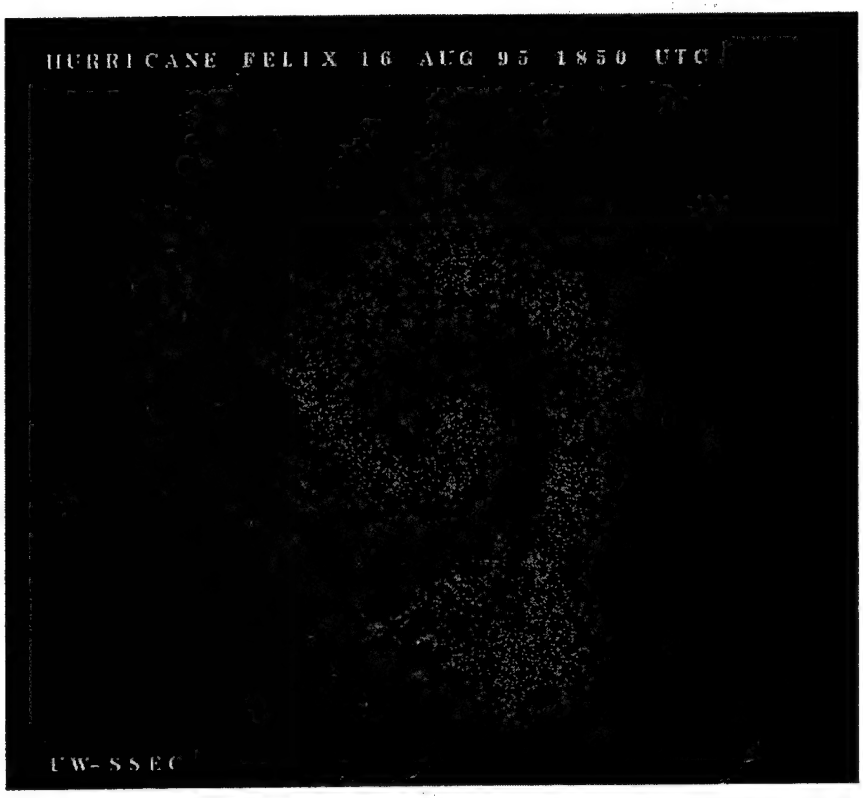

Fig. 19

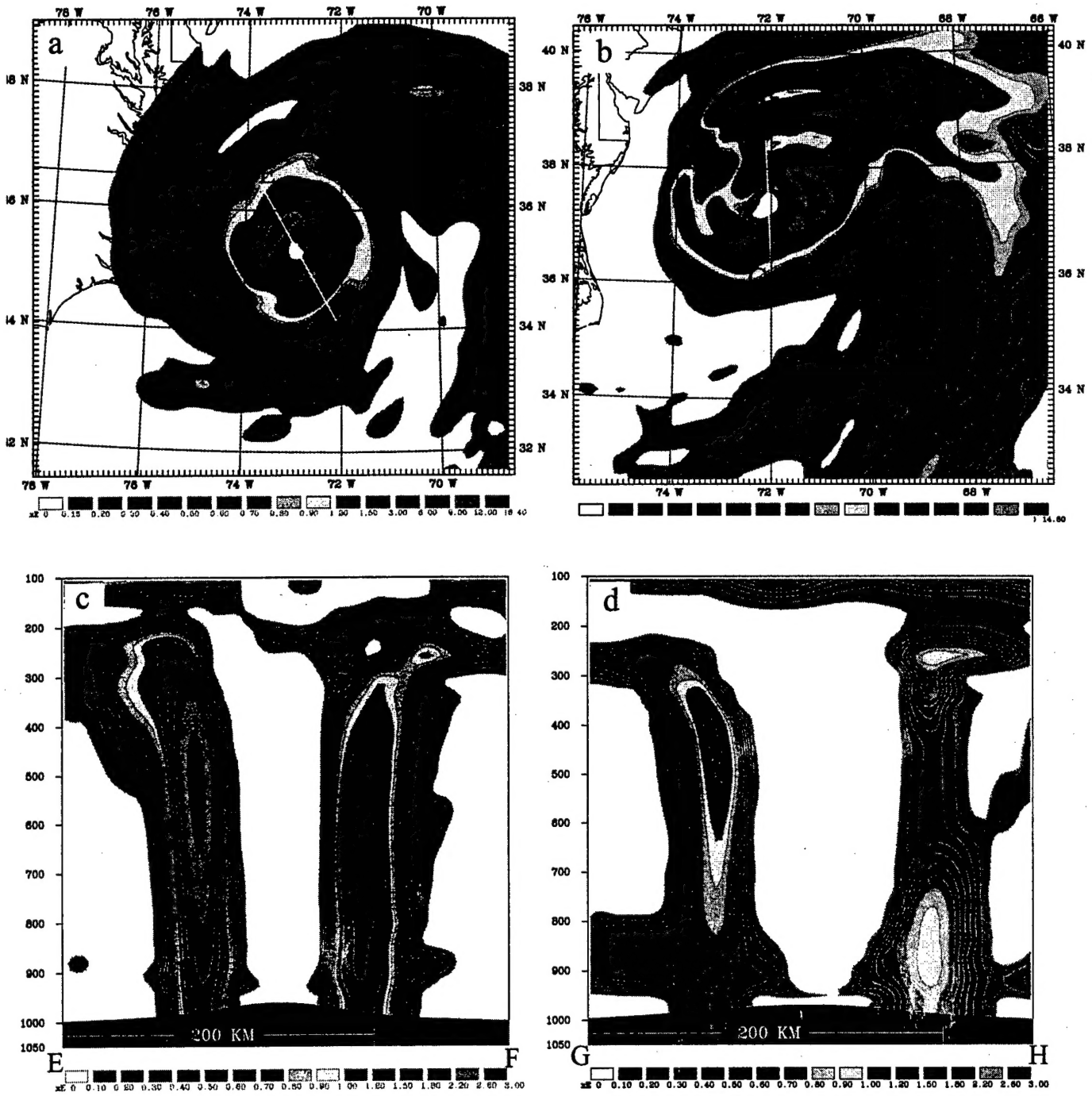

Fig. 20

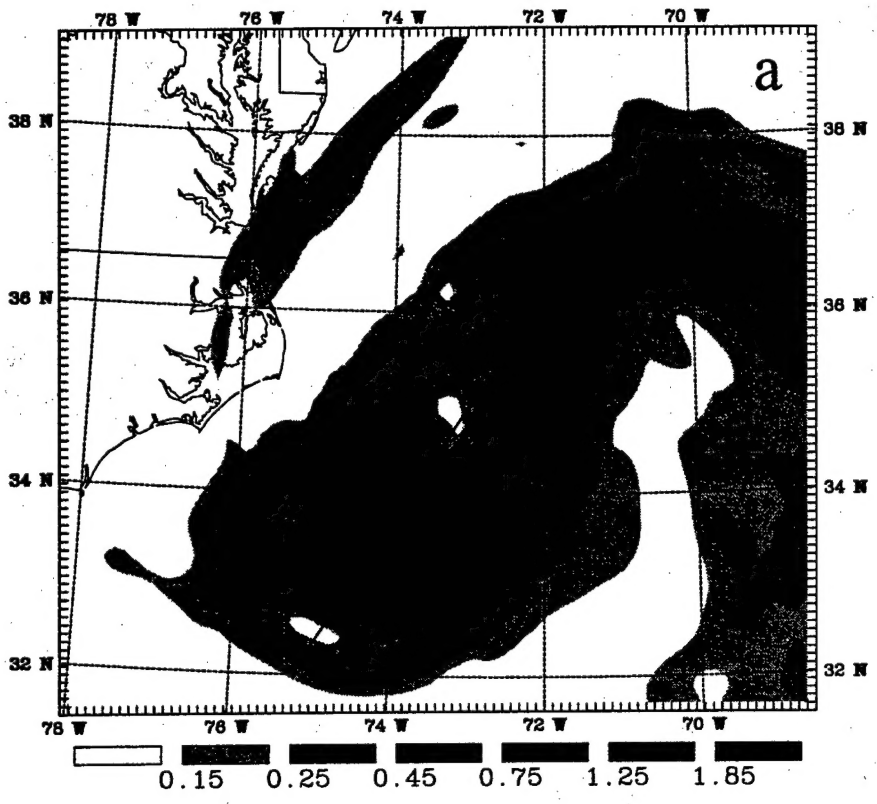
78 W
76 W
74 W
72 W
70 W
38 N
36 N
34 N
32 N
a
0.15
0.25
0.45
0.75
1.25
1.85

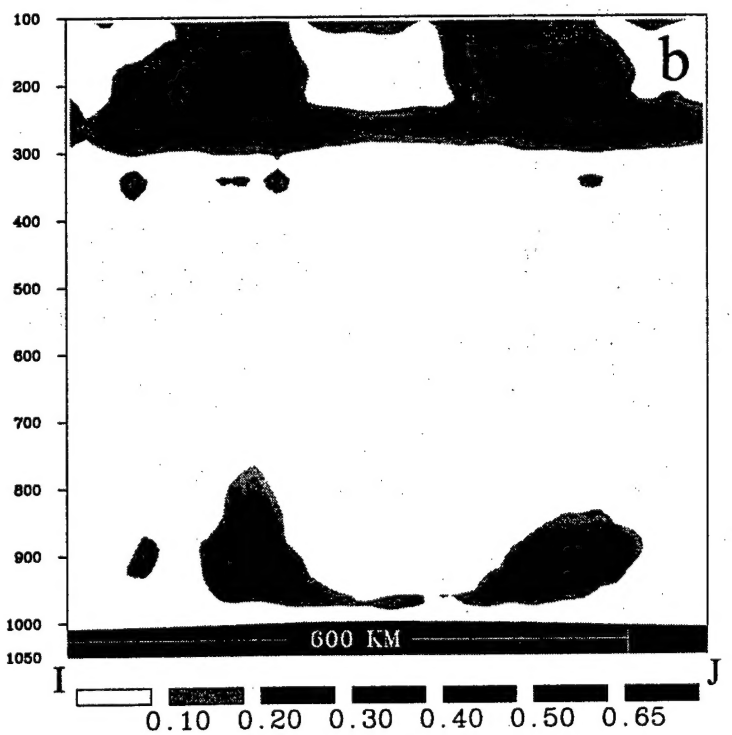
100
200
300
400
500
600
700
800
900
1000
1050
b
600 KM
I
J
0.10
0.20
0.30
0.40
0.50
0.65

Fig.21

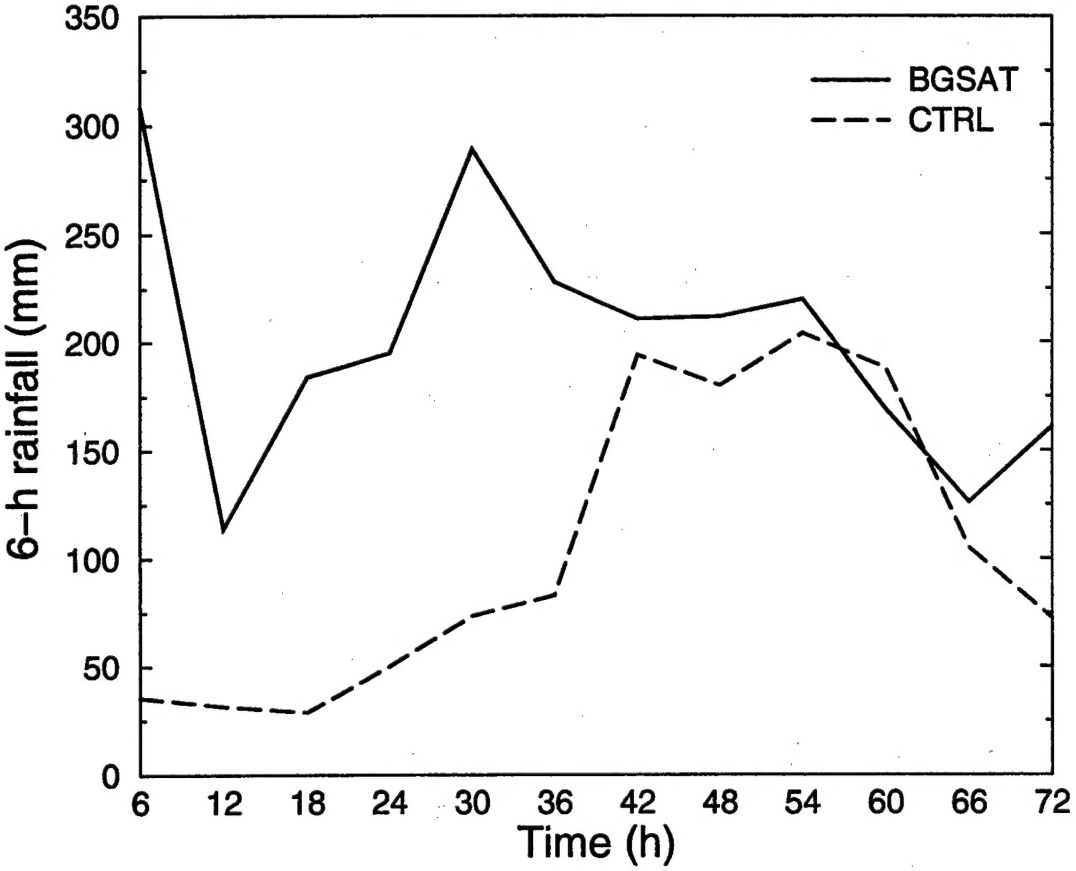
350
300
250
200
150
100
50
0
6–h rainfall (mm)
BGSAT
CTRL
6
12
18
24
30
36
42
48
54
60
66
72
Time (h)

Fig.22

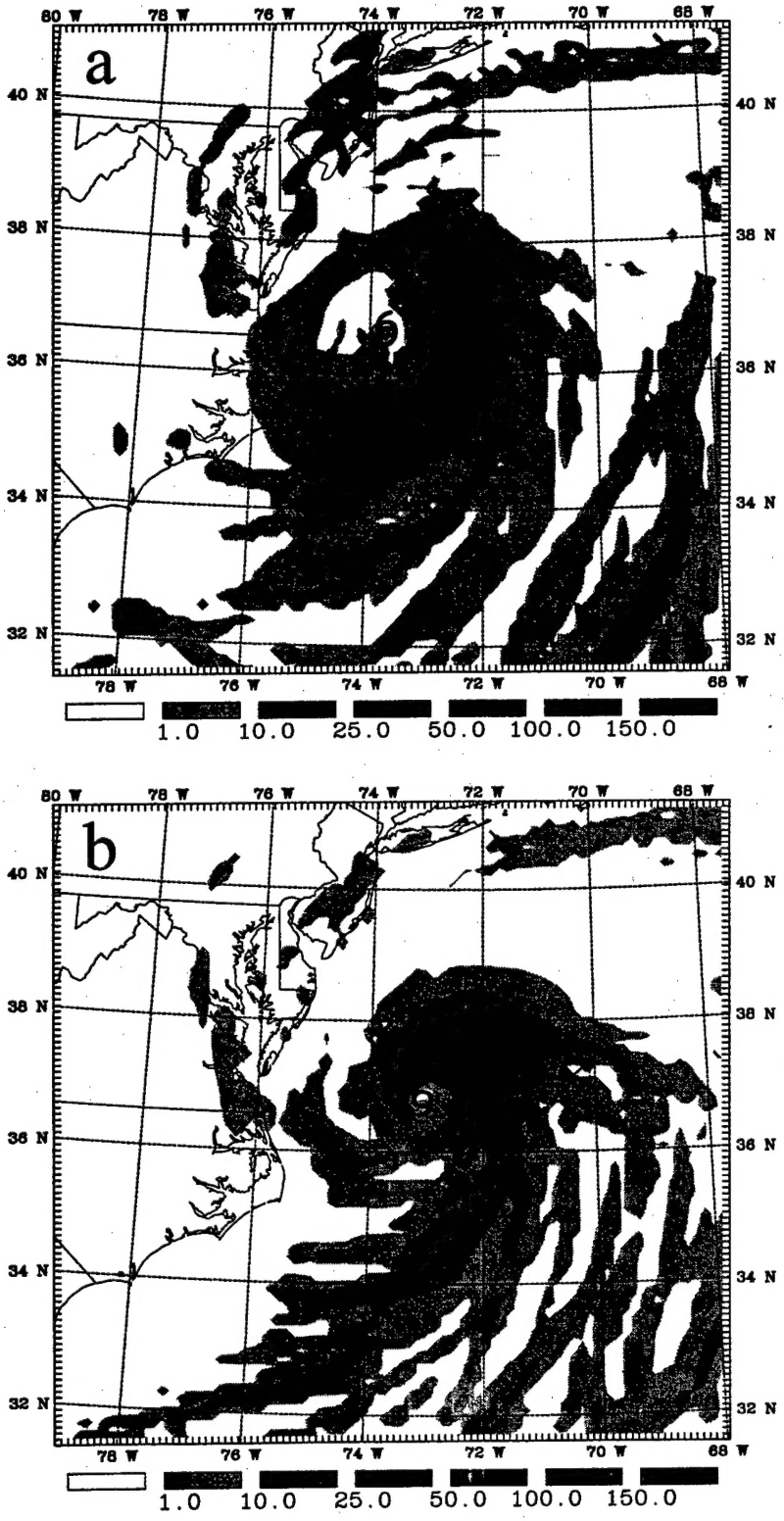
a
b
80 W
78 W
76 W
74 W
72 W
70 W
68 W
40 N
38 N
36 N
34 N
32 N
1.0
10.0
25.0
50.0
100.0
150.0

Fig. 23